JEM Journal of Experimental Medicine

ARTICLE

Early Notch signals from fibroblastic reticular cells program effector CD8⁺ T cell differentiation

Dave Maurice De Sousa[1,2,3*], Eric Perkey[4*], Laure Le Corre[1,2,3*], Salix Boulet[1], Daniela Gómez Atria[5], Anneka Allman[5], Frédéric Duval[1], Jean-François Daudelin[1], Joshua D. Brandstadter[5], Katlyn Lederer[5], Sarah Mezrag[1,2,3], Livia Odagiu[1,2], Myriam Ennajimi[1,2], Marion Sarrias[1,2], Hélène Decaluwe[6], Ute Koch[7], Freddy Radtke[7], Burkhard Ludewig[8], Christian W. Siebel[9], Ivan Maillard[5,10], and Nathalie Labrecque[1,2,3,11]

A better understanding of the mechanisms regulating CD8⁺ T cell differentiation is essential to develop new strategies to fight infections and cancer. Using genetic mouse models and blocking antibodies, we uncovered cellular and molecular mechanisms by which Notch signaling favors the efficient generation of effector CD8⁺ T cells. Fibroblastic reticular cells from secondary lymphoid organs, but not dendritic cells, were the dominant source of Notch signals in T cells via Delta-like1/4 ligands within the first 3 days of immune responses to vaccination or infection. Using transcriptional and epigenetic studies, we identified a unique Notch-driven T cell–specific signature. Early Notch signals were associated with chromatin opening in regions occupied by bZIP transcription factors, specifically BATF, known to be important for CD8⁺ T cell differentiation. Overall, we show that fibroblastic reticular cell niches control the ultimate molecular and functional fate of CD8⁺ T cells after vaccination or infection through the delivery of early Notch signals.

Introduction

Following antigen recognition, naïve CD8⁺ T cells massively expand and differentiate into effector cells endowed with the ability to control infection. This differentiation process involves a complex molecular cascade of events where external signals from antigen presentation, costimulation, and inflammation are integrated to orchestrate chromatin reorganization and induction of a transcriptional program that will generate, at the peak of the response, two main subsets of effector T cells: short-lived effector cells (SLECs) and memory precursor effector cells (MPECs) (Kaech et al., 2003; Joshi et al., 2007; Sarkar et al., 2008). Most SLECs die during the contraction phase of the response, while MPECs differentiate into long-lived memory CD8⁺ T cells (Kaech et al., 2003; Joshi et al., 2007; Sarkar et al., 2008). CD8⁺ T cell effector differentiation is regulated by several competing transcription factors: T-BET, ID2, ZEB2, and BLIMP-1 that induce the SLEC transcriptional program, while EOMES, ID3, ZEB1, and BCL-6 favor MPEC differentiation (Intlekofer et al., 2005; Yang et al., 2011; Omilusik et al., 2015; Dominguez et al., 2015; Rutishauser et al., 2009; Kallies et al., 2009; Ji et al., 2011; Guan et al., 2018; Ichii et al., 2002). Shortly after T cell activation, binding sites for RUNX, basic leucine zipper domain (bZIP), and NR4A family members are among the first motifs to become more accessible in chromatin (Wang et al., 2018). While NR4A transcription factors and the bZIP family member BACH2 are viewed as molecular breaks of CD8⁺ T cell function (Odagiu et al., 2020; Liu et al., 2019; Chen et al., 2019), this first wave of transcription factor activity results in further increases in chromatin accessibility and in the establishment of a collaborative molecular network driving differentiation. For example, BATF and IRF4 collaborate to bind DNA and synergize with RUNX3 and T-BET to restructure chromatin architecture and establish the effector program (Kurachi et al., 2014; Tsao et al., 2022). In addition, RUNX3 increases transcription of *Irf4* and *Prdm1* (encoding BLIMP-1) and promotes accessibility to memory regulatory regions (Wang et al., 2018). We and others showed that Notch pathway activation controls SLEC differentiation, but how the pathway interacts with the SLEC/MPEC transcription factor network remains unknown

[1]Maisonneuve-Rosemont Hospital Research Center, University of Montreal, Montreal, Canada; [2]Institut de Recherches Cliniques de Montréal, Montreal, Canada; [3]Département de Microbiologie, Infectiologie et Immunologie, Université de Montréal, Montreal, Canada; [4]Graduate Program in Cellular and Molecular Biology, University of Michigan, Ann Arbor, MI, USA; [5]Perelman School of Medicine, University of Pennsylvania, Philadelphia, PA, USA; [6]Cytokines and Adaptive Immunity Laboratory, CHU Sainte-Justine Research Center, Montreal, Canada; [7]École Polytechnique Fédérale de Lausanne, Lausanne, Switzerland; [8]Institute of Immunobiology, Kantonsspital St. Gallen, St. Gallen, Switzerland; [9]Genentech, South San Francisco, CA, USA; [10]Memorial Sloan Kettering Cancer Center, New York, NY, USA; [11]Département de Médecine, Université de Montréal, Montreal, Canada.

Correspondence to Nathalie Labrecque: nathalie.labrecque@umontreal.ca; Ivan Maillard: maillai@mskcc.org

*D. Maurice De Sousa, E. Perkey, and L. Le Corre are co-first authors.

(Mathieu et al., 2015; Backer et al., 2014). Furthermore, Notch was described as an amplifier of SLEC differentiation by integrating and positively feeding into SLEC-driving signals such as IL-2 and AKT/mTOR (Backer et al., 2014; Kalia et al., 2010; Obar et al., 2010; Macintyre et al., 2011; Araki et al., 2009; Kim et al., 2012). Indeed, IL-2 and mTOR can modulate Notch receptor expression in CD8⁺ T cells, while Notch expression is required for full induction of these pathways, as measured by CD25 expression and AKT/mTOR phosphorylation (Backer et al., 2014; Mathieu et al., 2015; Maurice De Sousa et al., 2019). Molecularly, when and how Notch fits in the complex network of transcription factors that regulate T cell differentiation remains unclear.

Notch influences the development and function of multiple immune cell types (Radtke et al., 2013; Amsen et al., 2015; Vanderbeck and Maillard, 2021). Notch is activated upon Notch receptor binding with ligands of the Delta-like (DLL) or Jagged family. Ligand-receptor interactions lead to receptor cleavage and release of the Notch intracellular domain (NICD), which translocates to the nucleus, associates with RBPJ, and recruits a member of the Mastermind-like (MAML) family and other co-activators to induce gene transcription (Osborne and Minter, 2007). Notch1 and Notch2 are present at low abundance in naïve CD8⁺ T cells, but their expression is induced following TCR stimulation and inflammation (Fiorini et al., 2009; Backer et al., 2014; Mathieu et al., 2013). During CD8⁺ T cell responses to vaccination and infection, we and others showed that Notch1 and Notch2 promote SLEC differentiation (Mathieu et al., 2015; Backer et al., 2014) through interactions with DLL1 and DLL4 Notch ligands (Perkey et al., 2020). Several studies showed that dendritic cell (DC) activation leads to increased Notch ligand expression (Amsen et al., 2004; Maekawa et al., 2008; Ito et al., 2009; Skokos and Nussenzweig, 2007; Napolitani et al., 2005; Mochizuki et al., 2013, 2016; Backer et al., 2014), suggesting that DCs can be sources of Notch ligands during T cell responses. Recent studies showed that DLL4 expression in secondary lymphoid organ fibroblastic reticular cells (FRCs) regulates T follicular cell (Tfh) differentiation, while DLL1 and DLL4 in FRCs drive T cell pathogenicity during graft-versus-host disease (GVHD) (Fasnacht et al., 2014; Chung et al., 2017). These findings raise the possibility that DLL1 and DLL4 expression by FRCs dictate in vivo CD8⁺ T cell fate. FRCs function as the specialized building blocks of lymphoid organ niches providing topological cues to support CD8⁺ T cell differentiation, as well as other cell types (Fasnacht et al., 2014; Camara et al., 2019; Bellomo et al., 2020; Perez-Shibayama et al., 2020; Cupovic et al., 2021; Alexandre et al., 2022). Recent observations indicate that FRC niches also sustain T cell activity in human lymphoid tissues (De Martin et al., 2023). Altogether, activated CD8⁺ T cells may receive Notch signals from activated DCs, FRCs, or both. Identifying the timing of Notch signaling and the cellular source(s) of Notch ligands is necessary to fill an important knowledge gap.

In this manuscript, we explore the temporal regulation as well as the cellular and molecular effects of Notch signaling in CD8⁺ T cell responses. Secondary lymphoid organ FRCs, and not hematopoietic antigen-presenting cells (APCs), provided critical Notch signals to CD8⁺ T cells to promote SLEC differentiation. The major effects of Notch on CD8⁺ T cells relied on signals delivered during the first 3 days of T cell activation. Transcriptomic analysis demonstrated that the Notch-regulated gene program in T cells was distinct from previously identified Notch signatures. Combined transcriptomic and epigenetic studies prior to the peak of the response showed that Notch activation was associated with enhanced chromatin opening, particularly at bZIP binding sites, leading to full induction of the T cell effector program and suppression of gene expression associated with the naïve T cell state. Finally, BATF but not c-JUN or JUNB overexpression promoted SLEC differentiation in Notch-deficient CD8⁺ T cells, suggesting that the activity of a restricted subset of bZIP family members was facilitated by Notch activation in this process. Together, our results integrate cellular, temporal, and molecular features of Notch activation to elucidate how it promotes differentiation of cytotoxic T cells.

Results

Notch ligand–dependent CD8⁺ T cell instruction by FRCs

We previously showed that DLL1- and DLL4-mediated activation of Notch1 and Notch2 receptors in CD8⁺ T cells promotes SLEC differentiation (Mathieu et al., 2015; Perkey et al., 2020). However, the cellular sources of Notch ligands during acute CD8⁺ T cell responses remain unknown. Several lines of evidence point to a role for Notch ligands in DCs, as their expression is induced during DC maturation (Amsen et al., 2004; Maekawa et al., 2008; Ito et al., 2009; Skokos and Nussenzweig, 2007; Napolitani et al., 2005; Mochizuki et al., 2013, 2016; Backer et al., 2014). The role of DC Notch ligands was never tested during CD8⁺ T cell differentiation in response to vaccination and infection in vivo. On the other hand, DLL1 and DLL4 are expressed by FRCs in secondary lymphoid organs, which emerged as critical cellular sources of Notch ligands during Tfh cell differentiation and alloimmune T cell responses in GVHD (Fasnacht et al., 2014; Chung et al., 2017; Perkey et al., 2020; Tkachev et al., 2023). Therefore, we evaluated whether DLL1 and DLL4 expression by FRCs was required for SLEC differentiation. We turned to Ccl19-Cre⁺*Dll1*$^{fl/fl}$*Dll4*$^{fl/fl}$ mice (referred to as *Dll1/4*$^{\Delta/\Delta}$, with Cre negative controls as *Dll1/4*$^{fl/fl}$) specifically lacking DLL1 and DLL4 expression in secondary lymphoid organ FRCs (Chai et al., 2013; Cremasco et al., 2014; Rodda et al., 2015; Chung et al., 2017). We vaccinated *Dll1/4*$^{\Delta/\Delta}$ versus *Dll1/4*$^{fl/fl}$ mice with ovalbumin (OVA) peptide–pulsed bone marrow (BM)–derived DCs (BMDCs) differentiated with FLT3L as these cells expressed high-level of DLL4 following TLR-induced maturation while GM-CSF BMDCs did not (Fig. S1 A) (Mochizuki et al., 2016). FLT3L-DCs were generated from the BM of control wild-type (WT) Mx1-Cre⁻*Dll1*$^{fl/fl}$*Dll4*$^{fl/fl}$ mice (referred to as DC fl/fl), or from DLL1 and DLL4-deficient BM from Mx1-Cre⁺*Dll1*$^{fl/fl}$*Dll4*$^{fl/fl}$ mice (referred to as DC Δ/Δ), both harvested from mice previously treated with poly(I:C) to induce Cre expression. This strategy inactivates *Dll1* and *Dll4* in all hematopoietic cells (Chung et al., 2017; Perkey et al., 2020). Antigen-pulsed WT and DLL1/4-deficient FLT3L-DCs were then used to vaccinate WT or Ccl19-Cre⁺*Dll1*$^{fl/fl}$*Dll4*$^{fl/fl}$ mice (respectively referred to as stromal fl/fl or stromal Δ/Δ) to delineate the essential cellular source of Notch ligands (Fig. 1 A). Abrogation of DLL1 and DLL4 expression

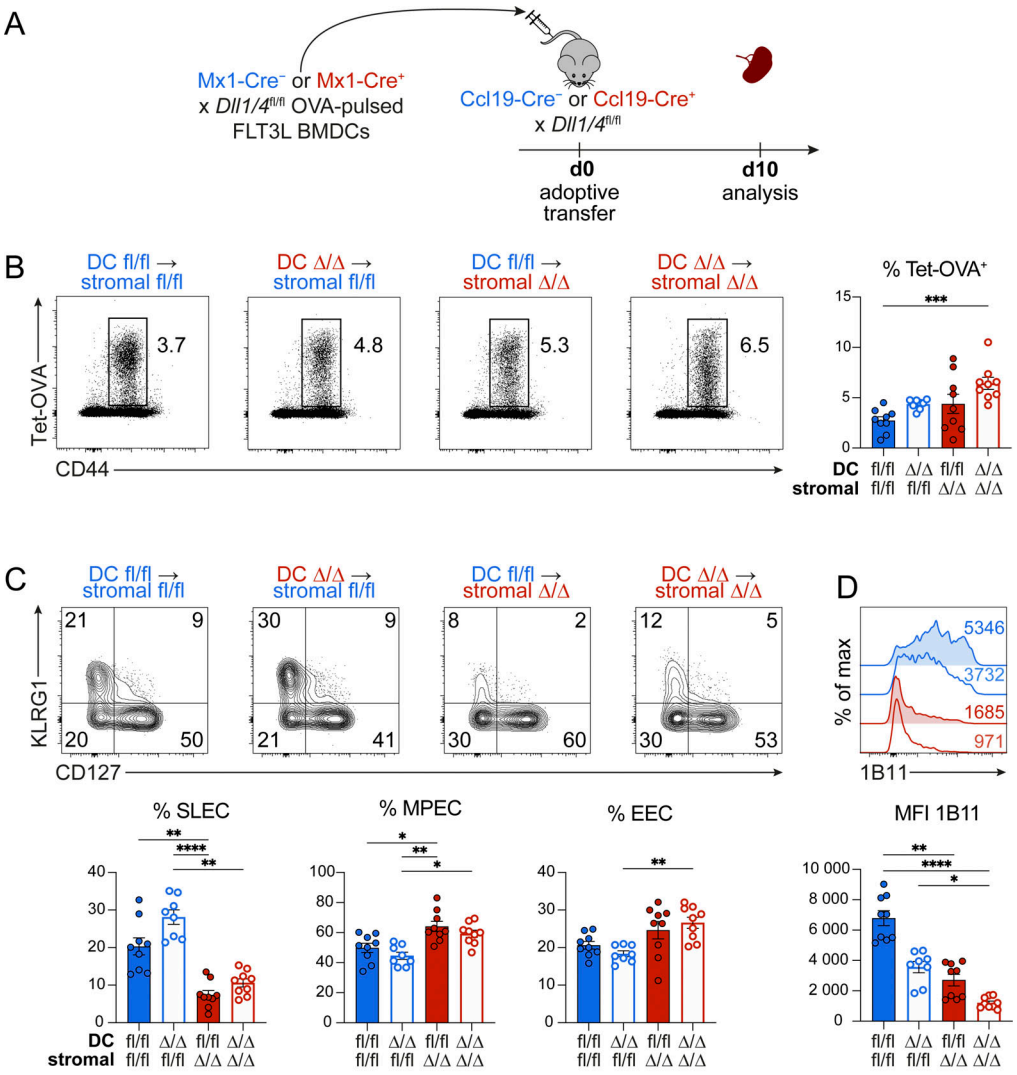

Figure 1. **Following vaccination, fibroblastic reticular cells but not DCs provide Notch signals to promote effector CD8⁺ T cell differentiation. (A–D)** Mice with or without a specific loss of Notch ligands DLL1/4 in stromal cells (Ccl19-Cre$^{+/-}$ × *Dll1*$^{fl/fl}$-*Dll4*$^{fl/fl}$) were vaccinated with OVA-loaded FLT3L BMDCs generated from poly(I:C)-treated Mx-Cre⁺ or Mx-Cre⁻ × *Dll1*$^{fl/fl}$-*Dll4*$^{fl/fl}$ mice to evaluate the respective roles of DLL1/4 on FLT3L-generated BMDCs and Ccl19-Cre⁺ stromal cells in CD8⁺ T cell expansion (B), SLEC/MPEC differentiation (C), and Notch-regulated GCNT1 activity detected by 1B11 staining (D). C and D are gated on Tet-OVA⁺ CD8⁺ T cells. Data are from two independent experiments with a total of n = 8–9 mice per group. Error bars display means ± SEM. Kruskal–Wallis ANOVA with Dunn's multiple comparison was used for multiple group comparison. *P < 0.05, **P < 0.01, ***P < 0.001, ****P < 0.0001.

in either stromal cells or DCs did not impact the overall expansion of OVA-specific CD8⁺ T cells after vaccination (Fig. 1 B) but profoundly decreased SLEC differentiation, while loss of DLL1 and DLL4 expression in DCs did not affect SLECs (Fig. 1 C). Cre expression alone in FRCs did not decrease the relative abundance of SLECs after DC vaccination (data not shown). To validate that FRCs were the major source of DLL1 and DLL4 for SLEC differentiation, we vaccinated WT or Ccl19-Cre⁺*Dll1*$^{fl/fl}$*Dll4*$^{fl/fl}$ mice (respectively referred to as stromal fl/fl or stromal Δ/Δ) and treated them with anti-DLL1 and anti-DLL4 blocking antibodies (Fig. S1 B). A similar OVA-specific CD8⁺ T cell expansion was observed in all mice (Fig. S1 C). SLEC differentiation was abrogated in mice lacking DLL1/4 expression in FRCs and this was not further decreased by anti-DLL1/4 treatment (Fig. S1 D). Furthermore, a similar decrease in SLEC differentiation was observed in mice with T cells expressing a dominant negative form of MAML1 (DNMAML), a potent inhibitor of canonical RBPJ/MAML-dependent Notch signaling (Maillard et al., 2004) (Fig. S1 E). To determine the intensity of Notch signaling experienced by CD8⁺ T cells, we leveraged our previous finding that *Gcnt1* is a Notch-regulated gene and that GCNT1-mediated core 2 glycosylation activity can be quantified via the detection of core 2-modified CD43 with the 1B11 antibody (Perkey et al., 2020). As evidenced by 1B11 staining, *Dll1/4* inactivation in FRCs resulted in decreased Notch signaling intensity in OVA-specific CD8⁺ T cells, while *Dll1/4* inactivation only in DCs had non-significant effects (Fig. 1 D). In the absence of DLL1 and DLL4 expression by secondary lymphoid organ FRCs, anti-DLL1/4 treatment decreased 1B11 staining when compared with the isotype control group (Fig. S1 F). Our results demonstrate an essential role for DLL1 and DLL4 expression by FRCs during CD8⁺ T cell differentiation into SLECs following DC

vaccination, although other cell types were able to contribute in a minor way to Notch signaling in CD8⁺ T cells as revealed with 1B11 reactivity as a sensitive readout.

Essential Notch ligand provision by FRCs during *Listeria* infection

Vaccination with DCs induces low levels of inflammation and SLEC generation when compared with infection (Badovinac et al., 2005). Inflammatory and TLR signals have been reported to induce Notch ligand expression in DCs (Ito et al., 2009; Skokos and Nussenzweig, 2007; Amsen et al., 2004; Napolitani et al., 2005; Mochizuki et al., 2013; Backer et al., 2014). We evaluated whether DLL1 and DLL4 expression was induced in DCs following *Listeria monocytogenes* (Lm) infection. *Dll1* and *Dll4* mRNA increased in DCs on day 2 after infection (Fig. S1 G). We then assessed whether Notch signals were provided by secondary lymphoid organ FRCs in the context of *Listeria* infection and its associated inflammation. We infected control versus Ccl19-Cre⁺*Dll1*$^{fl/fl}$*Dll4*$^{fl/fl}$ mice with Lm-OVA (expressing OVA as a model antigen) and analyzed OVA-specific CD8⁺ T cell response 7 days later. OVA-specific CD8⁺ T cell expansion was not impaired by *Dll1* and *Dll4* inactivation in FRCs (Fig. 2 A). Similarly, CD8⁺ T cell expansion was not impaired or even increased upon *Notch1/2* inactivation in CD8⁺ T cells (Fig. 2 A). The CD8⁺ T cell effector functions (Fig. S1 H), or bacterial control (not shown), were not affected by the inactivation of *Dll1* and *Dll4* in FRCs like previously reported for *Notch1/2* inactivation in CD8⁺ T cells (Mathieu et al., 2015). In contrast, SLEC differentiation was compromised by DLL1/4 loss in FRCs to a similar extent as previously reported for the loss of Notch1/2 receptors in CD8⁺ T cells (Fig. 2 B) (Mathieu et al., 2015). Furthermore, induction of 1B11 staining of core 2-modified CD43 in CD8⁺ T cells was dependent on DLL1/4 expression by FRCs (Fig. 2 C). These results establish the essential role of DLL1 and DLL4 expression by secondary lymphoid organ FRCs to trigger Notch signaling in T cells during their response to *Listeria* infection.

A recent study identified *Pofut1* as a regulator of Notch signals in CD8⁺ T cells. Similar to Notch-deficient T cells, CD8⁺ T cells lacking *Pofut1* showed decreased SLECs with a selective loss of effectors highly expressing CX3CR1 (Huang et al., 2021), raising the possibility that Notch signaling specifically affects the generation of CX3CR1^{hi} SLECs. Indeed, mice lacking DLL1/4 in secondary lymphoid organ FRCs showed loss of CX3CR1^{hi}CXCR3^{lo} SLECs after *Listeria* infection (Fig. 2 D), although to a lower extent than mice lacking *Notch1* and *Notch2* in CD8⁺ T cells (Fig. 2 D). This may result from strain differences (genetic and/or microbiome) or from Notch ligand–expressing cells not targeted by Ccl19-Cre that contribute to some extent to CX3CR1^{hi}CXCR3^{lo} SLEC differentiation.

In other contexts, signals provided by DLL ligands are often not redundant. This is illustrated by the observation that knocking in *Dll4* into the *Dll1* locus is embryonic lethal (Preuße et al., 2015). In GVHD, DLL4 is the main driver of IFN-γ production by alloreactive CD4⁺ T cells (Tran et al., 2013). Furthermore, DLL4 expression in FRCs regulates Tfh differentiation in lymph nodes, while DLL1 controls marginal zone B (MZB) cell homeostasis in the spleen (Fasnacht et al., 2014). To determine if DLL1 and DLL4 were both required for SLEC differentiation, we injected anti-DLL1 and anti-DLL4 antibodies in Lm-OVA–infected mice either separately or in combination. Anti-DLL1 or anti-DLL4 alone had only minor effects on the proportion of SLECs, while combined DLL1/4 blockade significantly decreased SLEC differentiation (Fig. 2 E). DLL1/4 inhibition did not affect overall effector functions (Fig. S1 I). The recapitulation of the SLEC phenotype by anti-DLL1/4 treatment demonstrates that Cre expression alone in FRCs did not impair SLEC differentiation. Thus, both DLL1 and DLL4 contributed to Notch signaling during effector CD8⁺ T cell differentiation, and secondary lymphoid organ Ccl19-Cre⁺ FRCs were the predominant source of these ligands for CD8⁺ T cells.

We then assessed whether memory CD8⁺ T cells generated in the absence of Notch signaling had a decreased ability to differentiate into SLECs following a secondary challenge. Notch signaling was also required to generate SLEC during a recall response (Fig. S2). Furthermore, WT memory CD8⁺ T cells were impaired in the generation of secondary SLECs when mice were treated with anti-DLL1/4 antibodies only during rechallenge with Lm-OVA (Fig. S2).

Notch provides early fate-determining signals during CD8⁺ T cell differentiation

To decipher the molecular events regulated by Notch signaling during CD8⁺ T cell responses, it is critical to identify when Notch signaling is provided to CD8⁺ T cells and when it impacts SLEC differentiation. We first defined the expression kinetics of Notch1 and Notch2. Notch receptor expression was measured by flow cytometry after the adoptive transfer of CD45.2⁺ OT-I cells into CD45.1⁺ recipients followed by Lm-OVA infection. Expression of Notch1 on primed antigen-specific CD8⁺ T cells was maximal on day 2 after infection and decreased by day 7 (Fig. 3 A). In contrast, cell surface Notch2 was not detected on antigen-specific CD8⁺ T cells during CD8⁺ T cell response (Fig. S3 A). This may be a consequence of transendocytosis of the extracellular domain of Notch following ligand engagement. Therefore, we used an antibody that targets the intracellular domain of Notch2 (NT/ICD2). NT/ICD2 detection followed a similar pattern as Notch1 (Fig. 3 A). For both receptors, staining specificity was validated using adoptive transfer of OT-I T cells with *Notch1* and *Notch2* gene inactivation (Fig. S3 B). As both Notch1 and Notch2 expression was induced on antigen-specific CD8⁺ T cells, we tested the role of individual Notch receptors during SLEC formation. We studied the immune response to Lm-OVA in mice with CD8⁺ T cells lacking expression of *Notch1* (E8I-Cre⁺-*Notch1*$^{fl/fl}$), *Notch2* (E8I-Cre⁺-*Notch2*$^{fl/fl}$), or both receptor genes (E8I-Cre⁺-*Notch1*$^{fl/fl}$*Notch2*$^{fl/fl}$). *Notch1* or *Notch2* inactivation alone had no impact on effector CD8⁺ T cell differentiation, while combined *Notch1/2* inactivation decreased SLEC proportion (Fig. 3 B). The lack of effect of single gene deletions demonstrates that Cre expression in CD8⁺ T cells was not responsible for the SLEC phenotype. Altogether, these results suggest that Notch signaling can occur throughout the expansion phase of the CD8⁺ T cell response to promote SLEC differentiation with a contribution of both Notch1 and Notch2.

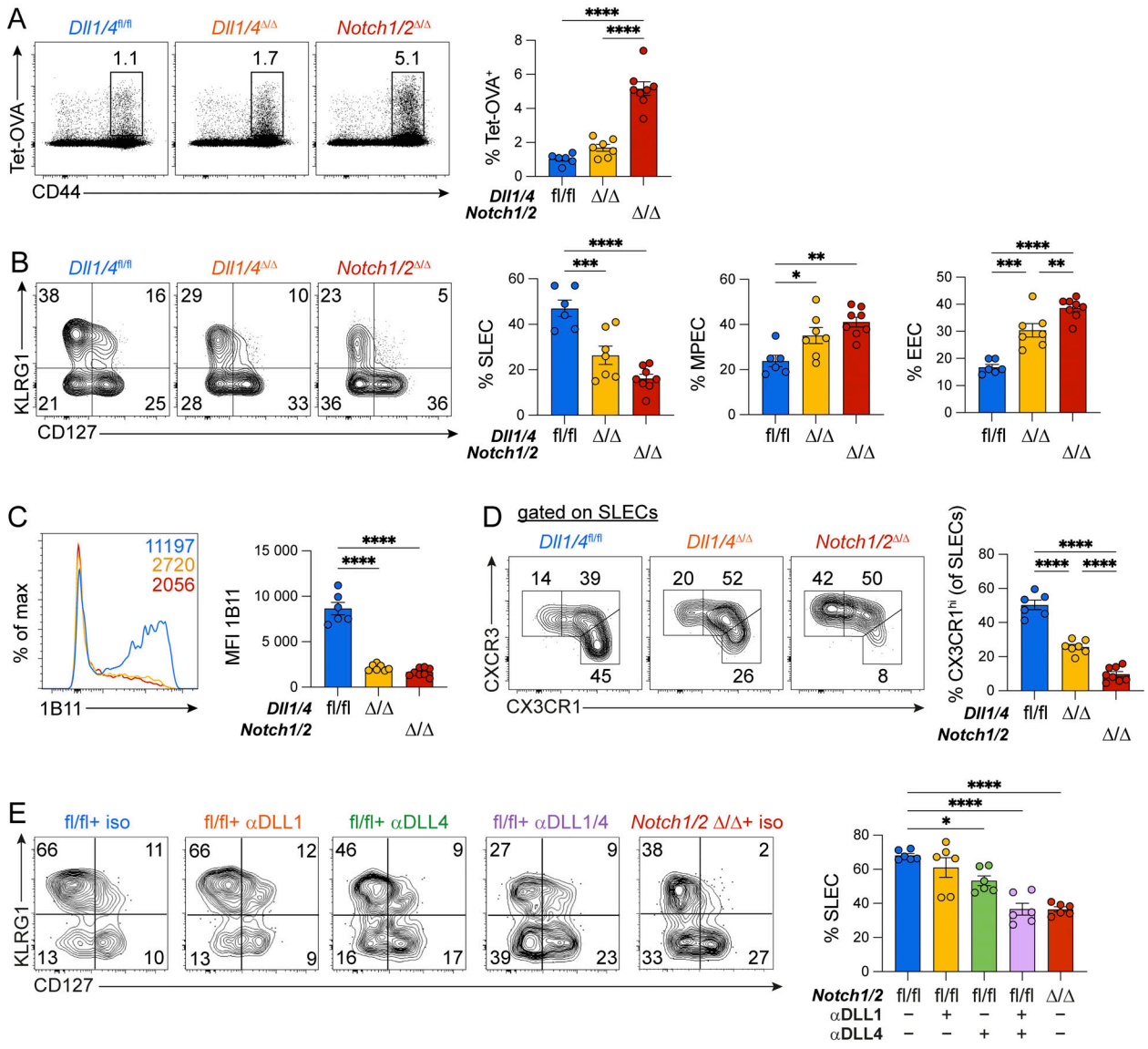

Figure 2. **Fibroblastic reticular cells from secondary lymphoid organs provide Notch signals to promote effector CD8⁺ T cell differentiation during infection.** Control (Ccl19-Cre⁻-*Dll1/4*$^{fl/fl}$; referred to as *Dll1/4*$^{fl/fl}$) or mice with a specific loss of Notch ligands DLL1 and DLL4 in FRCs (Ccl19-Cre⁺-*Dll1/4*$^{fl/fl}$; referred to as *Dll1/4*$^{Δ/Δ}$) were infected with Lm-OVA. As a comparison, *Notch1/2* KO (E8I-Cre⁺*Notch1/2*$^{fl/fl}$) mice were included. The CD8⁺ T cell response was assessed 7 days later in the spleen by flow cytometry. **(A)** Representative plots (left) and compilation (right) of the OVA-specific polyclonal CD8⁺ T cell response detected by tetramer staining. **(B)** Representative plots (left) and compilation (right) of the proportion of SLECs, MPECs, and early effector cells (EECs) among Tet-OVA⁺ CD8⁺ T cells. **(C)** Binding of the 1B11 antibody to detect the core-2 *O*-glycosylated form of CD43 was used as a Notch signaling indicator on Tet-OVA⁺ cells from *Dll1/4*$^{fl/fl}$ and *Dll1/4*$^{Δ/Δ}$ mice following Lm-OVA infection. **(D)** Representative plots (left) and compilation (right) of the proportion of CX3CR1^{hi}CXCR3^{lo} SLECs from *Dll1/4*$^{fl/fl}$ and *Dll1/4*$^{Δ/Δ}$ mice following Lm-OVA infection. **(E)** WT mice were treated with an isotype control or blocking antibodies against DLL1, DLL4, or both on days 0 and 2 after Lm-OVA infection. The proportion of SLECs was measured among Tet-OVA⁺ CD8⁺ T cells. Data are from two independent experiments with a total of *n* = 6–8 mice per group (A–E). Error bars display means ± SEM. Ordinary one-way ANOVA with Tukey's multiple comparison was used for multiple group comparison. *P < 0.05, **P < 0.01, ***P < 0.001, ****P < 0.0001.

To evaluate when Notch signaling impacted the SLEC molecular program, we injected anti-DLL1/4 antibodies on day 0 and day 2 after infection with Lm-OVA or delayed the antibody injection to day 3.5 after infection, before assessing the response on day 7. Delayed injection of anti-DLL1/4 antibodies had a minor impact on SLEC differentiation, while DLL1/4 blockade on days 0 and 2 abrogated SLEC differentiation and recapitulated the phenotype of *E8I*-Cre⁺*Notch1*$^{fl/fl}$-*Notch2*$^{fl/fl}$ mice (Fig. 3 C). The effect on SLEC differentiation was partial with anti-DLL1/4 blockade on day 2 or 3 (Fig. S3 C). Decreased CX3CR1^{hi}CXCR3^{lo} SLECs and 1B11 expression were also observed following systemic antibody-mediated blockade of DLL1 and DLL4 (Fig. S3, D and E). Therefore, Notch signals delivered within the first 3 days of the immune response are essential to program SLEC differentiation.

Identifying when essential Notch signals were delivered to CD8⁺ T cells was critical to identifying a Notch-regulated signature most proximal to the transcriptional effects of the

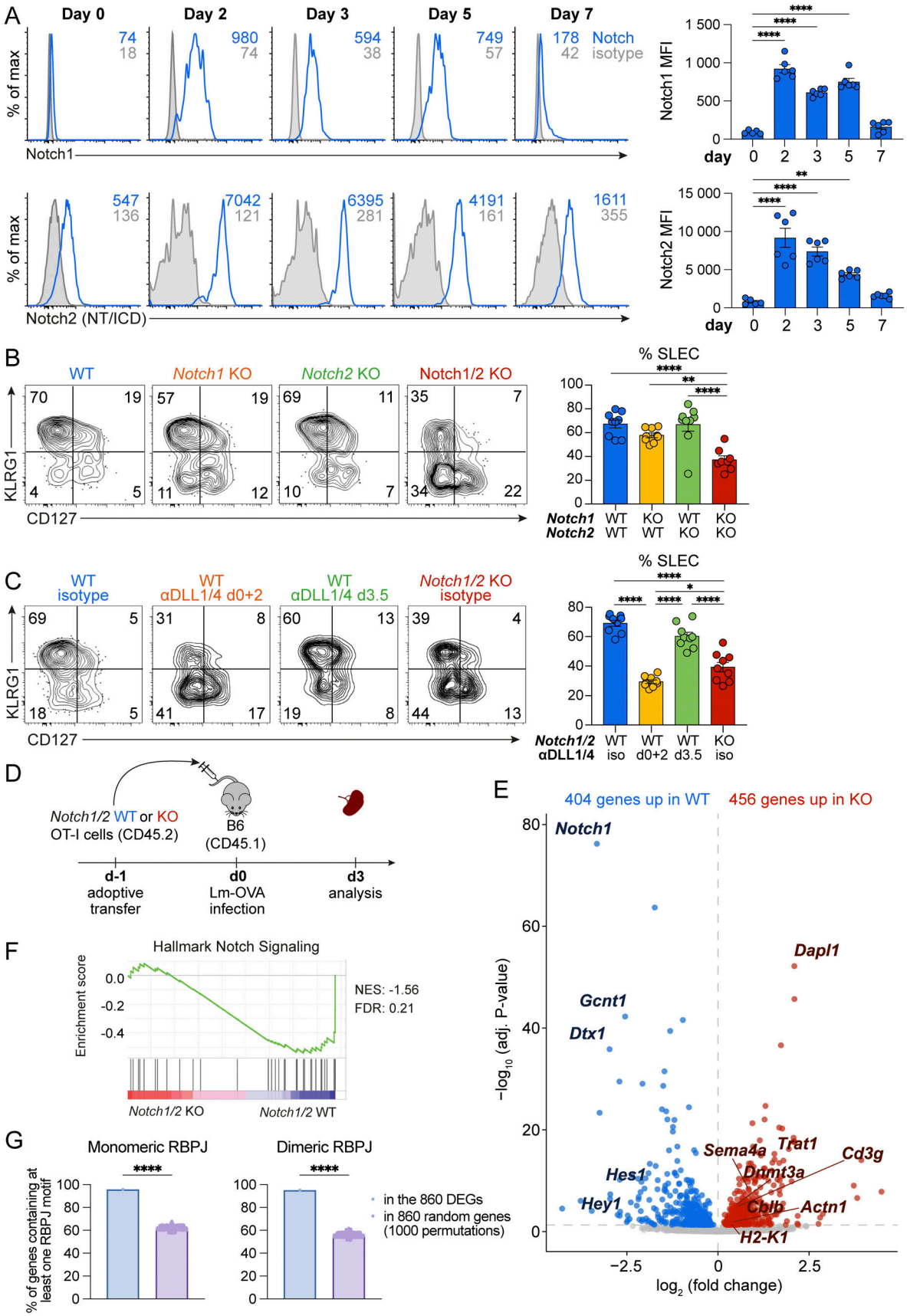

Figure 3. **Early Notch signals control SLEC differentiation and early transcriptional events in antigen-specific CD8⁺ T cells. (A)** Notch1 and Notch2 expression by OT-I CD8⁺ T cells was measured in naïve mice (gated on OT-I) or on days 2, 3, 5, and 7 (gated on OT-I CD44⁺) after infection with Lm-OVA.

(B) The redundancy of Notch signaling via Notch1 and Notch2 receptors was tested by measuring the proportion of OVA-specific SLECs following Lm-OVA infection in WT (E8I-Cre$^-$-*Notch1/2*$^{fl/fl}$), *Notch1* KO (E8I-Cre$^+$-*Notch1*$^{fl/fl}$), *Notch2* KO (E8I-Cre$^+$-*Notch2*$^{fl/fl}$), or both *Notch1/2* KO (E8I-Cre$^+$*Notch1/2*$^{fl/fl}$). **(C)** The consequence of early (days 0 and 2) or delayed (day 3.5 [d3.5]) inhibition of Notch signaling with anti-DLL1/4 antibodies on SLEC differentiation was assessed on day 7 after Lm-OVA infection. Gated on Tet-OVA$^+$ cells. **(D)** RNA-seq was performed on day 3 after infection to compare the transcriptomes of Notch WT (E8I-Cre$^-$-*Notch1/2*$^{fl/fl}$) and Notch KO (E8I-Cre$^+$-*Notch1/2*$^{fl/fl}$) OT-I cells. **(E)** Volcano plot of differentially expressed genes (adjusted P value <0.05). **(F)** GSEA showing the Hallmark Notch Signaling from MSigDB on RNA-seq data comparing Notch WT and KO OT-I cells on day 3 after infection. NES, normalized enrichment score; FDR, false discovery rate. **(G)** Enrichment of RBPJ binding motifs at DEGs. Data are from two independent experiments (A) or three independent experiments (B and C) with a total of n = 5–9 mice per group. Error bars display means ± SEM. Ordinary one-way ANOVA with Tukey's multiple comparison was used for multiple group comparison and unpaired two-tailed t test was used for two-group comparisons. *P < 0.05, **P < 0.01, ****P < 0.0001.

pathway. As very few antigen-specific T cells are present on day 3 after infection in a polyclonal repertoire, we adoptively transferred WT (*E8I*-Cre$^-$*Notch1*$^{fl/fl}$*Notch2*$^{fl/fl}$) versus *Notch1/2*-deficient (KO; *E8I*-Cre$^+$*Notch1*$^{fl/fl}$*Notch2*$^{fl/fl}$) OT-I CD8$^+$ T cells to B6-CD45.1 recipients and analyzed their transcriptome on day 3 after Lm-OVA infection (Fig. 3 D), prior to their acquisition of a SLEC phenotype, as illustrated by the lack of KLRG1 expression (Fig. S3 F). 860 gene transcripts were differentially expressed (Padj < 0.05) in WT versus *Notch1/2*-deficient CD8$^+$ T cells on day 3 after infection (Fig. 3 E). Amongst them, 217 transcripts had >1.5-fold change, with 115 genes showing downregulated and 102 upregulated expression in Notch-deficient CD8$^+$ T cells (Table S1). Known Notch target gene transcripts such as *Hes1*, *Dtx1*, and *Hey1* were decreased in the absence of Notch signaling (Fig. 3 E and Fig. S3 G). Furthermore, RPBJ binding motifs (monomeric and dimeric) were enriched within differentially expressed genes (DEGs) as compared with randomly selected genes (Fig. 3 G), suggesting that our transcriptome analysis on day 3 includes some genes that are potentially regulated by Notch. Gene set enrichment analysis (GSEA) of our RNA sequencing (RNA-seq) data showed only modest enrichment for the publicly available Hallmark Notch Signaling gene set from the Molecular Signature Database (MSigDB, Fig. 3 F), and this was driven in part by decreased *Notch1* and *Notch2* mRNA, the targets of our genetic modification (Subramanian et al., 2005). This was also reported in a dataset studying the role of the Notch pathway in CD4$^+$ T cells during GVHD (Chung et al., 2019). A prior comparison of Notch-dependent T-cell acute lymphoblastic leukemia (T-ALL), mantle cell lymphoma, and triple-negative breast cancer showed only a few shared Notch target genes but also many tumor and cell type-specific Notch-regulated genes (Petrovic et al., 2019). As classical Notch signatures available in public databases are derived from Notch-dependent tumors, our data suggest that Notch signaling in peripheral T cells regulates a distinct mature T cell–specific gene set.

Identification of a mature T cell–specific Notch transcriptional signature

To generate a reliable Notch signature for peripheral T cells, we combined our RNA-seq data with data from CD4$^+$ T cells in a GVHD model where Notch signaling was inhibited using anti-DLL1/4 antibodies (Chung et al., 2019). We selected these datasets because both were obtained at the early stages of the T cell response, when the action of the Notch pathway is critical (Chung et al., 2019); and this paper. Among DEGs (622 for CD4$^+$ T cells and 875 for CD8$^+$ T cells), we identified 82 genes with upregulated expression and 54 with downregulated expression in the absence of Notch signaling shared by both datasets (Fig. S4, A and B; and Table S2). Gene Ontology (GO) term analysis of gene transcripts decreased in the absence of Notch signaling (the Notch T cell signature) and suggested that in activated T cells, Notch regulated processes of cell adhesion and T cell differentiation. Notch-repressed genes were enriched for several terms related to the control of T cell responses, such as metabolism, interferon signaling, and defense response (Fig. S4 C). To further validate that our Notch T cell signature captures genes that are regulated directly by Notch signaling, we evaluated its enrichment in activated CD8$^+$ T cells that were co-cultured for 24 h on OP9 or OP9-DLL4. As shown in Fig. S4 D, the Notch T cell signature was enriched following a culture of activated CD8$^+$ T cells on OP9-DLL4.

We then compared the Notch T cell signature to Notch signatures defined in other contexts, such as BM progenitors or acute T cell lymphoblastic leukemia (GO term Notch Signaling Pathway; GSEA-Vilimas: BM progenitors overexpressing the NICD; GSEA Notch hallmarks: computationally derived signature; (Wang et al., 2011): CUTLL1 cell line + gamma secretase inhibitor [GSI] washout) (Gene Ontology Consortium et al., 2021; Vilimas et al., 2007; Subramanian et al., 2005; Wang et al., 2011). Interestingly, our Notch T cell signature was not enriched for these other Notch signatures (Fig. 4 A), with *Dtx1*, a known Notch target, being the only overlapping gene between all signatures. To validate the significance of our gene set across mature T cells in other contexts, we studied other existing transcriptomic data where Notch signaling was manipulated in T cells. These included the transcriptome of WT and *Notch1/2*-deficient CD8$^+$ T cells on day 10 after infection with influenza (Backer et al., 2014), WT and *Notch1/2*-deficient T helper type 2 cells (Th2) effectors challenged in vivo with an allergen (Tindemans et al., 2020), and T regulatory cells with/without overexpression of the constitutively active NICD (Charbonnier et al., 2015). Enrichment analysis by mROAST (Wu et al., 2010) showed that genes with upregulated expression in the absence of Notch signaling in our signature were enriched in conditions with decreased Notch signaling (Fig. 4 B and Table S3). Conversely, genes with downregulated expression in the absence of Notch signaling in our signature were enriched by enhanced Notch activity (Fig. 4 B). Moreover, our Notch T cell signature allowed for clustering of both CD4$^+$ or CD8$^+$ T cells receiving or not Notch signals (Fig. S4 E). We also tested the signature using RNA-seq data from T cells in which we did not expect Notch signaling to be active (naïve CD8$^+$ T cells and in vitro cultured

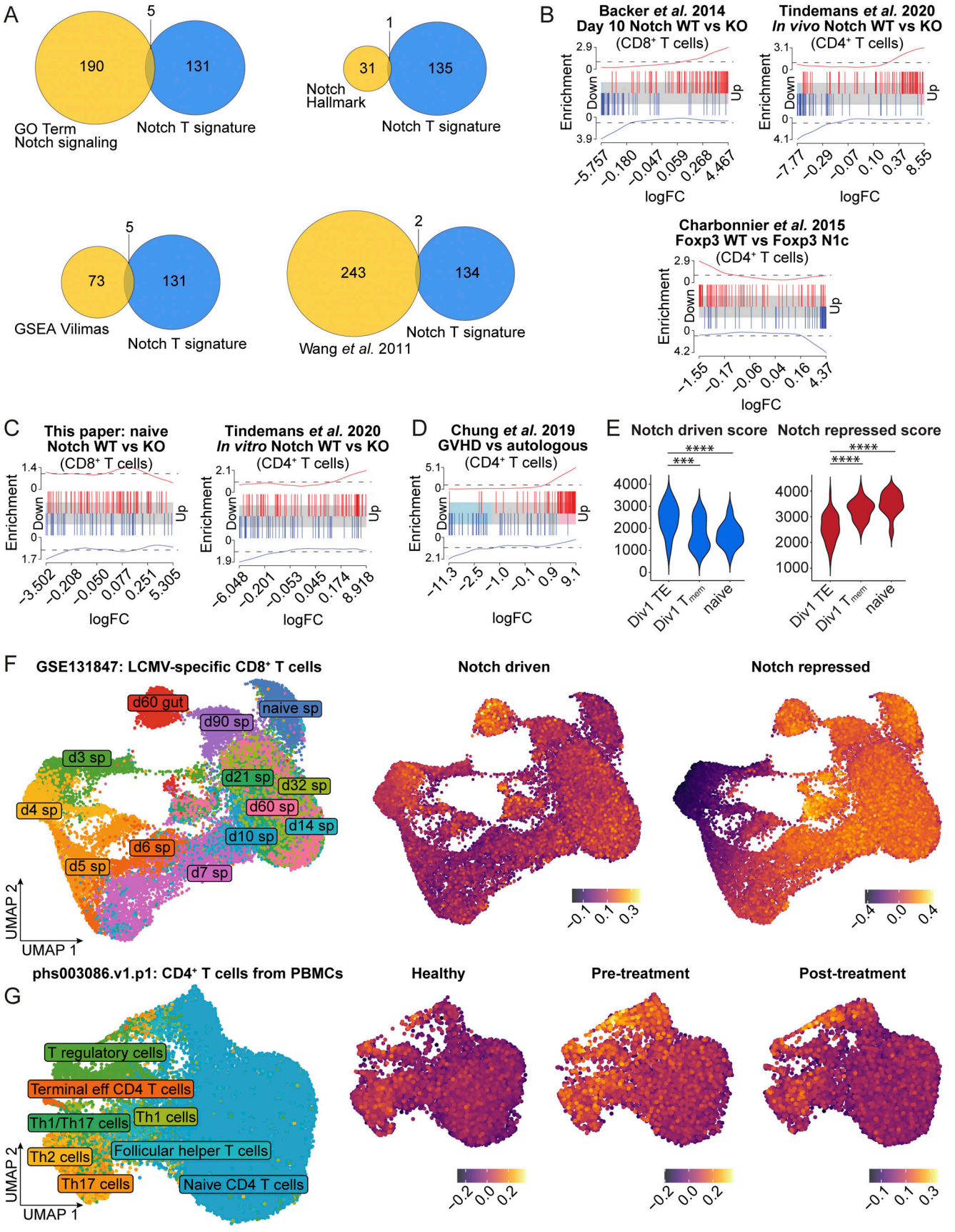

Figure 4. **Identification of a T cell–specific Notch transcriptional signature.** A T cell–specific Notch signature was obtained by selecting differentially expressed genes with similar expression patterns in activated CD4+ (GSE126518) and CD8+ (this paper) T cells that had received or not received Notch signals.

(A) Venn diagram illustrating the overlap of the Notch T cell signature with currently available Notch signatures: GO term Notch signaling, the Vilimas gene set from MSigDB (both up and down), the Notch Hallmark gene set from MSigDB, and Notch1 target genes from Wang et al. (2011). **(B–D)** mROAST enrichment analysis for the T cell–specific Notch signature across indicated publicly available datasets. **(E)** Enrichment scores of Notch-driven and Notch-repressed signatures were determined in available scRNA-seq data from P14 CD8⁺ T cells that had undergone a single cell division following LCMV Armstrong infection (Kakaradov et al., 2017). **(F)** UMAP projection of available scRNA-seq data (GSE131847) from P14 cells in the spleen (sp) and gut at different time points after LCMV Armstrong infection. Each cell is colored by day of isolation and tissue (left) or by the relative expression of the genes from the Notch T cell signature that are either induced (middle) or downregulated (right) by the Notch pathway. **(G)** scRNA-seq data (Benamar et al., 2023) from healthy controls or MIS-C patients was reanalyzed; cells automatically labeled as CD4 were selected and visualized by UMAP (left). The relative expression level of the Notch gene signature is shown in each group (right). Ordinary one-way ANOVA with Tukey's multiple comparisons was used for multiple group comparison. ***P < 0.001, ****P < 0.0001.

cells). We did not observe significant enrichment for our Notch T cell signature (Fig. 4 C and Table S3). These data suggest that our Notch T cell signature can identify T cells receiving Notch signals in different contexts and differentiation states.

Although several reports, including our own, showed potent biological effects of Notch on different aspects of T cell differentiation (Chung et al., 2017, 2019; Zhang et al., 2011; Tran et al., 2013; Mathieu et al., 2015; Backer et al., 2014; Tindemans et al., 2020; Charbonnier et al., 2015; Fasnacht et al., 2014), enrichment for the Hallmark Notch signature in transcriptomic studies of CD4⁺ and CD8⁺ T cell responses has seldom been reported. Our data suggest that previously available Notch signatures are not adequate to interrogate mature T cells. We thus evaluated if our newly described Notch T cell signature was enriched during different types of T cell responses. As early Notch signaling plays a critical role during the induction of GVHD (Tran et al., 2013), we tested whether the Notch T cell signature was enriched in CD4⁺ alloreactive compared with syngeneic T cells at 48 h after transfer (Chung et al., 2019). Indeed, the T cell Notch signature was highly enriched in alloreactive T cells (Fig. 4 D and Table S3). We also tested whether the Notch T cell signature was linked to early T cell fate determination in single-cell RNA-seq (scRNA-seq) data from sorted LCMV-specific P14 TCR transgenic CD8⁺ T cells that had undergone a single cell division in response to LCMV Armstrong (Kakaradov et al., 2017). The score of genes with an expression pattern driven by Notch was higher in cells from the first division with an effector profile, while the score of genes suppressed by Notch was lower in the same population (Fig. 4 E). This is consistent with early Notch signaling activity during effector T cell differentiation. Finally, we evaluated whether the Notch T cell signature was detectable during CD8⁺ T cell responses to infection in publicly available scRNA-seq data (Kurd et al., 2020; Milner et al., 2020). The activity of the upregulated and downregulated Notch T cell signature was strongest in antigen-specific CD8⁺ T cells early in the response (days 3 and 4), but not later (Fig. 4 F). This corroborates our data demonstrating that Notch plays an essential role in the first 3 days after activation for optimal SLEC generation. Furthermore, the Notch-driven signature was enriched in LCMV-specific CD8⁺ T cells in the gut on day 30 (Fig. 4 F), consistent with a reported role of Notch signaling in CD103⁺ resident memory CD8⁺ T cells (Hombrink et al., 2016). Our Notch T cell signature was also enriched in CD4⁺ T cells, particularly regulatory T cells, from SARS-CoV-2-infected children with multisystem inflammatory syndrome (MIS-C) associated with dominant negative mutations in NUMB and NUMBL that lead to increased NOTCH1 expression (Fig. 4 G), while the classical Notch signature was not enriched (Benamar et al., 2023). These data demonstrate the value of our newly defined Notch T cell signature to probe diverse T cell responses in mice and humans.

Notch-regulated genes are enriched in molecular pathways associated with cytokine responsiveness

While the T cell Notch signature uncovered information about molecular pathways regulated by Notch in mature T cells, it did not explain the effects of Notch signaling on MPEC/SLEC differentiation. Among the 860 gene transcripts that were differentially abundant ($P_{adj} < 0.05$) in WT and Notch-deficient CD8⁺ T cells on day 3 after infection (Fig. 3 E), several are known to influence SLEC/MPEC differentiation, such as *Il2ra*, *Prdm1*, *Bach2*, *Tcf7*, and *Id3* (Fig. 5 A) (Kalia et al., 2010; Rutishauser et al., 2009; Kallies et al., 2009; Roychoudhuri et al., 2016; Zhou et al., 2010; Ji et al., 2011; Yang et al., 2011). To get further insights, we analyzed differentially expressed genes in Notch-sufficient versus Notch-deprived CD8⁺ T cells ($P_{adj} < 0.05$ and $|\log_2 FC| > 1$) using DAVID GO molecular functions (Dennis et al., 2003). In agreement with the similar recovery of WT and N1N2 KO (*E8I*-Cre⁺*Notch1*$^{fl/fl}$*Notch2*$^{fl/fl}$) OT-I effectors and no difference in cell death markers (Fig. S3, H and I), cell survival and cell death molecular pathways were not enriched in our dataset. Cytokine and chemokine receptor activity as well as cytokine binding were among the most significantly affected pathways (Fig. 5 B). Analysis of upstream regulators via ingenuity pathway analysis (IPA) further supported Notch-mediated regulation of genes controlling cytokine responsiveness, as 15 of the 25 upstream regulators were cytokines and STATs, with the top one being IL-2 (Fig. 5 C). The possible impact of Notch on IL-2 signaling was in line with previous observations that sustained T cell CD25 expression was reduced in the absence of Notch signaling (Zhang et al., 2011; Backer et al., 2014; Mathieu et al., 2015).

To determine the cytokine signaling pathway(s) affected by Notch deficiency in CD8⁺ T cells, we harvested activated OT-I T cells obtained on day 3 following Lm-OVA infection, stimulated them with IL-2, IL-15, or IL-21, and measured STAT phosphorylation (STAT5 for IL-2 and IL-15; STAT3 for IL-21; and STAT4 for IL-12). Only STAT5 phosphorylation after IL-2 stimulation was affected in Notch-deficient OT-I T cells (Fig. 5 D). Reduced phospho-STAT5 (p-STAT5) correlated with decreased CD25 cell surface expression (Fig. 5 E). Amongst CD25^{hi} cells, Notch1/2 WT and KO OT-I T cells had similar levels of p-STAT5, suggesting that decreased p-STAT5 was a consequence of

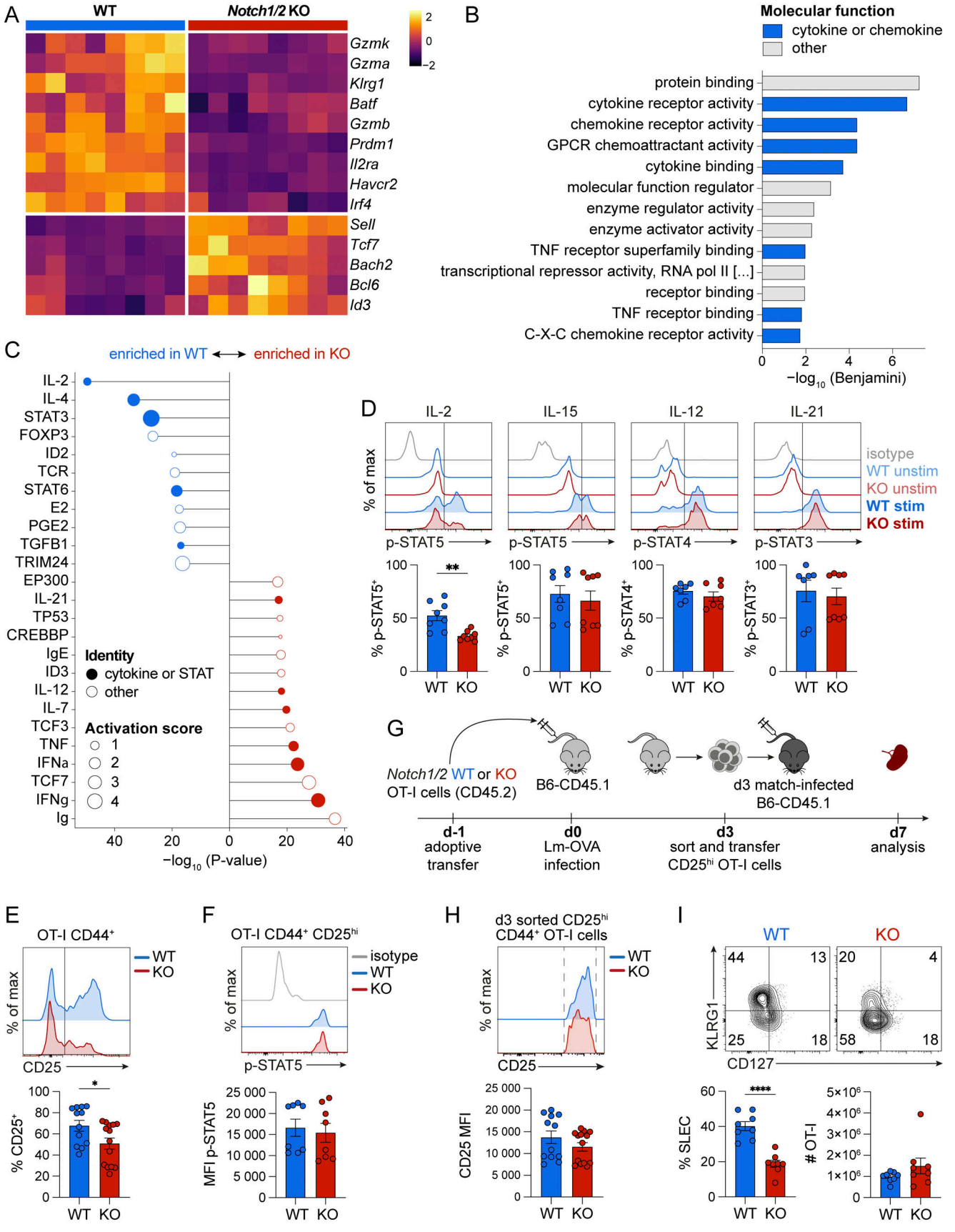

Figure 5. **Suboptimal IL-2 signaling in Notch-deficient CD8⁺ T cells is not the sole contributor to defective SLEC differentiation. (A)** Transcription of genes involved in SLEC/MPEC differentiation or effector functions by day 3 effector CD8⁺ T cells (data from RNA-seq). **(B)** Cytokine-related GO terms enriched

in the differentially expressed genes between Notch WT and KO OT-I effectors. **(C)** Top 25 significant upstream regulators in our dataset were determined by IPA. **(D)** On day 3 after Lm-OVA infection, WT or Notch KO OT-I cells were stimulated ex vivo for 30 min with IL-2, IL-15, IL-12, or IL-21, and the phosphorylation of the appropriate STAT molecules was measured by flow cytometry (STAT5, STAT5, STAT4, and STAT3, respectively). Isotype control for cytokine-stimulated cells and staining of unstimulated cells are also shown. **(E)** Representative plots (top) and compilation (bottom) of the expression of the IL-2 receptor α chain (CD25) at day 3 after infection on Notch-sufficient and Notch-deficient CD8$^+$ T cells. **(F)** Representative plots (top) and compilation (bottom) of pSTAT5 levels in OT-I CD44$^+$CD25^{hi} cells following in vitro IL-2 restimulation on day 3 after infection. **(G)** Experimental design for the adoptive transfer of Notch WT or KO CD25^{hi} OT-I cells into match-infected recipients on day (d) 3 after infection. **(H)** CD25 expression on sorted CD25^{hi} CD44$^+$ OT-I cells from Notch WT and KO at day 3 after Lm-OVA infection (related to Fig. 5 H). **(I)** At d7 after infection, differentiation of the transferred CD25^{hi} OT-I CD8$^+$ T cells into SLECs was evaluated in the spleen by flow cytometry. Representative plots and compilation of SLEC proportions and OT-I cell recovery. Data are from two independent experiments (D–I) with a total of n = 7–14 mice per group. Error bars display means ± SEM. Unpaired two-tailed t test was used for two-group comparisons. *P < 0.05, **P < 0.01, ****P < 0.0001.

decreased CD25 expression in Notch-deficient T cells and not of defective intracellular signaling downstream of the IL-2 receptor (Fig. 5 F).

To assess if Notch signaling enhanced SLEC differentiation via induction of CD25 expression, we sorted WT (E8I-Cre$^-$*Notch1*$^{fl/fl}$*Notch2*$^{fl/fl}$) and KO (E8I-Cre$^+$*Notch1*$^{fl/fl}$*Notch2*$^{fl/fl}$) day 3 OT-I effector CD8$^+$ T cells expressing high levels of CD25 (Fig. 5 H), which have similar levels of p-STAT5 upon IL-2 stimulation (Fig. 5 F). These cells were adoptively transferred into matched-infected recipients (Fig. 5 G). 4 days after transfer, we still observed decreased SLEC generation by CD25^{hi} OT-I T cells lacking *Notch1* and *Notch2* as compared with Notch-sufficient OT-I T cells (Fig. 5 I) without any impact on cell recovery (Fig. 5 I). These findings suggest that the effects of Notch deficiency on SLEC differentiation extend beyond its impact on IL-2 signaling.

Notch activation increases chromatin accessibility of bZIP transcription factors

One mechanism by which Notch signaling could regulate SLEC differentiation is by regulating chromatin accessibility either directly or indirectly via induction of other transcription factors or regulators. In the context of T cell acute lymphoblastic leukemia, Notch activation is associated with increased deposition of H3K27Ac active enhancer marks at Notch target genes, with long-range effects on chromatin (Wang et al., 2011). Similar observations were reported in *Drosophila* for H3K56Ac (Skalska et al., 2015). The possible effect of Notch signaling on chromatin accessibility is further supported by Notch-mediated recruitment of the SWI/SNF complex, other chromatin remodeling factors, and epigenetic modulators (Pillidge and Bray, 2019; Schwanbeck et al., 2011; Wang et al., 2014; Takeuchi et al., 2007; Yatim et al., 2012; Kadam and Emerson, 2003; Ntziachristos et al., 2012). This body of work suggests that Notch has the potential to regulate chromatin remodeling, which is essential for naïve-to-effector CD8$^+$ T cell differentiation (Yu et al., 2017; Wang et al., 2018; Scott-Browne et al., 2016). To study the impact of Notch signaling on chromatin accessibility in activated CD8$^+$ T cells, we used the same approach and experimental time point as for transcriptomic analysis (Fig. 3 D). Using assay for transposase-accessible chromatin with sequencing (ATAC-seq), we identified 1,678 differentially accessible regions (DARs) in Notch WT versus KO CD8$^+$ T cells on day 3 after infection. Most of these DARs (68%) were more accessible in WT compared with KO (Fig. 6 A). The vast majority of DARs were found in introns as well as intergenic regions (Fig. 6 A), and they lay at least 10 kb from transcription start sites (TSS) (Fig. 6 B), implying that Notch activation in T cells mostly modulates chromatin accessibility at enhancers, and not at promoters.

HOMER and GREAT annotation tools (McLean et al., 2010; Heinz et al., 2010) associated these DARs with 2,282 genes. To elucidate the molecular network influenced by Notch signaling during early CD8$^+$ T cell differentiation, we compared RNA-seq and ATAC-seq data and identified 221 common genes between these datasets (Fig. 6 C). Among genes both epigenetically and transcriptionally regulated upon Notch activation, expression of the SLEC-associated genes *Il2ra*, *Prdm1*, and *Klrg1* was induced in Notch-sufficient cells, while that of MPEC-associated genes *Tcf7*, *Bach2*, and *Id3* was repressed (Fig. 6 D) (Kalia et al., 2010; Rutishauser et al., 2009; Kallies et al., 2009; Roychoudhuri et al., 2016; Zhou et al., 2010; Ji et al., 2011; Yang et al., 2011).

Transcription factor binding motif enrichment analysis using HOMER applied to our ATAC-seq data showed enrichment of DNA binding motifs for the bZIP family transcription factors in the more accessible WT DARs (Fig. S5 A). Footprinting analysis of the ATAC-seq data revealed enhanced binding of bZIP transcription factors in Notch-sufficient compared with KO CD8$^+$ T cells (Fig. 6 E and Fig. S5 B). These footprints for bZIPs were enriched in genes differentially expressed in WT versus *Notch1/2*-deficient CD8$^+$ T cells (Fig. S5 C). To determine if the enrichment for bZIP transcription factors could explain the impact of Notch on SLEC differentiation, we turned to data from Scott-Browne et al., who performed ATAC-seq analysis in several CD8$^+$ T cell subsets (Scott-Browne et al., 2016). Their findings revealed that DARs could be segregated into 12 different clusters showing selective enrichment in naïve, effector, SLEC, MPEC, memory, and exhausted CD8$^+$ T cells (Scott-Browne et al., 2016). Interestingly, these clusters were also selectively enriched for specific transcription factor binding motifs. Effector and SLEC-specific DARs were greatly enriched for binding motifs for bZIPs. Therefore, we classified DARs in our ATAC-seq data using the Scott-Browne et al. clustering. DARs that were more open in the presence of Notch signaling were far more likely to be distributed in the effector- and SLEC-specific clusters, which were enriched in bZIP motifs (Fig. 6 F). In contrast, accessible Notch KO DARs were enriched in naïve-specific clusters, which had no bZIP motif enrichment (Fig. 6 F). This further suggests that Notch activation controls SLEC differentiation by directly or indirectly potentiating the binding of bZIP transcription factors in chromatin regions important for SLEC differentiation. This

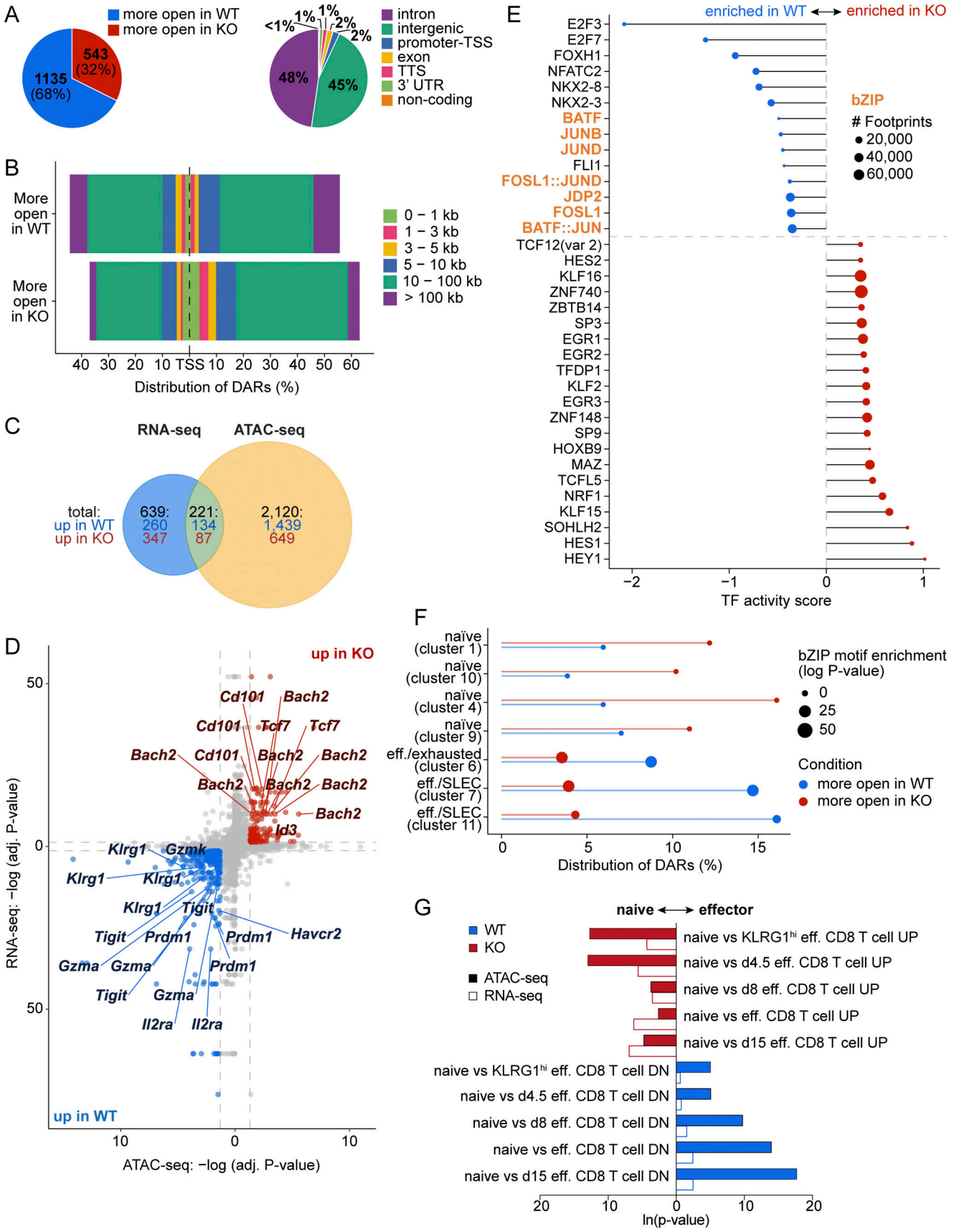

Figure 6. **Notch signaling increases chromatin accessibility of bZIP transcription factors during effector CD8⁺ T cell differentiation. (A)** 3 days after infection by Lm-OVA, Notch WT and KO OT-I CD44⁺ cells were collected for ATAC-seq. DARs were identified and distributed according to their genotype (left)

or genomic location (right). **(B)** DARs were associated with genes using the HOMER annotation tool before being distributed by distance from their TSS. **(C)** Common DEGs from our RNA-seq and gene-associated DARs (using HOMER and GREAT annotation tools) from our ATAC-seq were identified while conserving the directionality of the data. **(D)** Several Notch-regulated genes common to our RNA-seq and ATAC-seq and important for SLEC/MPEC differentiation or function are plotted. **(E)** Transcription factor (TF) footprinting analysis was performed on all identified ATAC-seq peaks using HINT-ATAC, and statistically significative enrichment ($P < 0.05$) in either Notch WT or KO was illustrated. Members of the bZIP family are represented in orange. **(F)** Notch DARs (this paper) were distributed in DAR clusters defined by Scott-Browne et al. (2016). bZIP motif enrichment, calculated by Scott-Browne et al. on their clusters, is also represented. **(G)** GSEA was performed on Notch DEGs and DARs. Several immunological signatures of naïve versus effector (eff.) CD8$^+$ T cells were enriched ($P < 0.05$). ATAC-seq experiment was performed in two independent adoptive transfers and infections (A–G).

scenario is supported by GSEA of our RNA-seq and ATAC-seq data, as Notch WT cells were enriched for effector CD8$^+$ T cell signatures, while Notch1/2 KO cells were enriched for naïve T cell signatures (Fig. 6 G). Our results suggest that Notch signaling acts early in activated CD8$^+$ T cells and is necessary to fully induce the effector program while repressing the transcription of naïve T cell–associated genes. This is associated with chromatin opening at enhancers, either directly by NICD or indirectly by other Notch-regulated transcription factors, resulting in increased binding of bZIP transcription factors to these regions.

BATF requires Notch signaling for the generation of CX3CR1^{hi} SLECs

BATF is a member of the bZIP family essential for naïve-to-effector CD8$^+$ T cell differentiation and expansion (Kurachi et al., 2014). BATF was recently described as an important epigenetic regulator of early effector CD8$^+$ T cell differentiation (Tsao et al., 2022). To evaluate if Notch cooperates with BATF to regulate CD8$^+$ T cell differentiation, we compared our RNA-seq with data reported by Tsao et al. in which WT and BATF KO CD8$^+$ T cells were analyzed on day 3.5 after LCMV Armstrong infection (Tsao et al., 2022). A significant fraction of DEGs were common to both transcriptomes, with 32% of the genes regulated by Notch also regulated by BATF (Fig. 7 A). We also observed an overlap in DARs affected by Notch and BATF (Fig. 7 B). Furthermore, the majority of DARs regulated by Notch were shown by others to be bound by BATF in in vitro–activated CD8$^+$ T cells (Fig. 7, C and D) and in vivo day 5 antigen-specific CD8$^+$ T cells (Fig. S5 D) (Tsao et al., 2022; McDonald et al., 2023).

To determine if Notch and bZIP transcription factors cooperate to induce SLEC differentiation, we overexpressed JUNB, c-JUN, or BATF using retroviral transduction in WT or Notch-deficient OT-I T cells before TCR activation (Fig. 7 E). Overexpression of BATF, but not JUNB and c-JUN, in Notch-deficient OT-I CD8$^+$ T cells increased SLEC proportions (Fig. 7, F and G). SLEC generation was also increased by BATF overexpression in WT OT-I CD8$^+$ T cells.

As Notch deficiency selectively affected the generation of CX3CR1^{hi} SLECs, we evaluated if BATF overexpression restored CX3CR1^{hi}CXCR3^{lo} SLECs in the absence of Notch signaling. BATF overexpression in Notch-deficient OT-I CD8$^+$ T cells was not sufficient to promote the generation of CX3CR1^{hi}CXCR3^{lo} SLECs (Fig. 8, A and B), similar to JUNB and c-JUN overexpression (not shown). To define whether BATF overexpression in Notch-deficient CD8$^+$ T cells was sufficient to rescue expression of the gene signature shared by BATF and Notch signaling, we performed RNA-seq analysis in Notch-sufficient or -deficient CD8$^+$ T cells overexpressing or not BATF on day 3 after infection with Lm-OVA. BATF overexpression was not sufficient to fully restore the expression of the gene sets that are both affected by Notch- and BATF deficiency (Fig. 8 C). Among genes whose expression was regulated by both Notch signaling and BATF, only one quarter (60/239) was rescued by BATF overexpression in Notch-deficient CD8$^+$ T cells indicating that without Notch signaling, BATF cannot control a large fraction of the common Notch-BATF-regulated genes (Fig. 8 C). The genes whose expression was modulated by BATF overexpression in Notch-deficient CD8$^+$ T cells were not enriched for the SLEC signature (Fig. 8 D). These data imply that Notch signaling is critical to allow the transcription of a subset of genes regulated by BATF during effector CD8$^+$ T cell differentiation with a key role in the generation of CX3CR1^{hi}CXCR3^{lo} SLECs. Altogether, our data suggest that BATF cannot induce the full program of effector CD8$^+$ T cell differentiation in the absence of Notch signaling.

Discussion

In this study, we elucidated the critical time points as well as cellular and molecular mechanisms by which Notch signaling controls SLEC differentiation. Our findings reveal that early Notch activation, instigated through T cell interactions with FRC niches, induces the expression of a CD8$^+$ T cell–specific Notch transcriptional signature. This process also correlates with increased chromatin accessibility at enhancers enriched for BATF binding sites.

We identified Ccl19-Cre$^+$ FRCs as the primary cellular source of DLL1 and DLL4 Notch ligands to orchestrate SLEC differentiation following both vaccination and acute infection, while other sources of Notch ligands may contribute to some Notch signals controlling the upregulation of 1B11 reactivity (a sensitive readout). The key role for DLL1 and DLL4 expression by Ccl19-Cre$^+$ FRCs to promote SLEC differentiation further expands the role of FRC niches in shaping CD8$^+$ T cell responses. Previous works showed that FRCs provide more than physical support and migration cues for T cell response in lymphoid organs (Onder et al., 2022). The production of IL-6 by FRCs promotes epigenetic remodeling in T cells to facilitate their survival and differentiation (Brown et al., 2019). Interestingly, binding motifs of bZIP transcription factors, including BATF, were enriched in chromatin regions that FRC–T cell interactions induce to open (Brown et al., 2019). Past work indicated that FRCs actively respond to inflammation and infection and that this response is necessary for proper T cell activation, expansion, and differentiation (Perez-Shibayama et al., 2020; Alexandre et al., 2022; De Martin et al., 2023). Our data demonstrate that one of the key

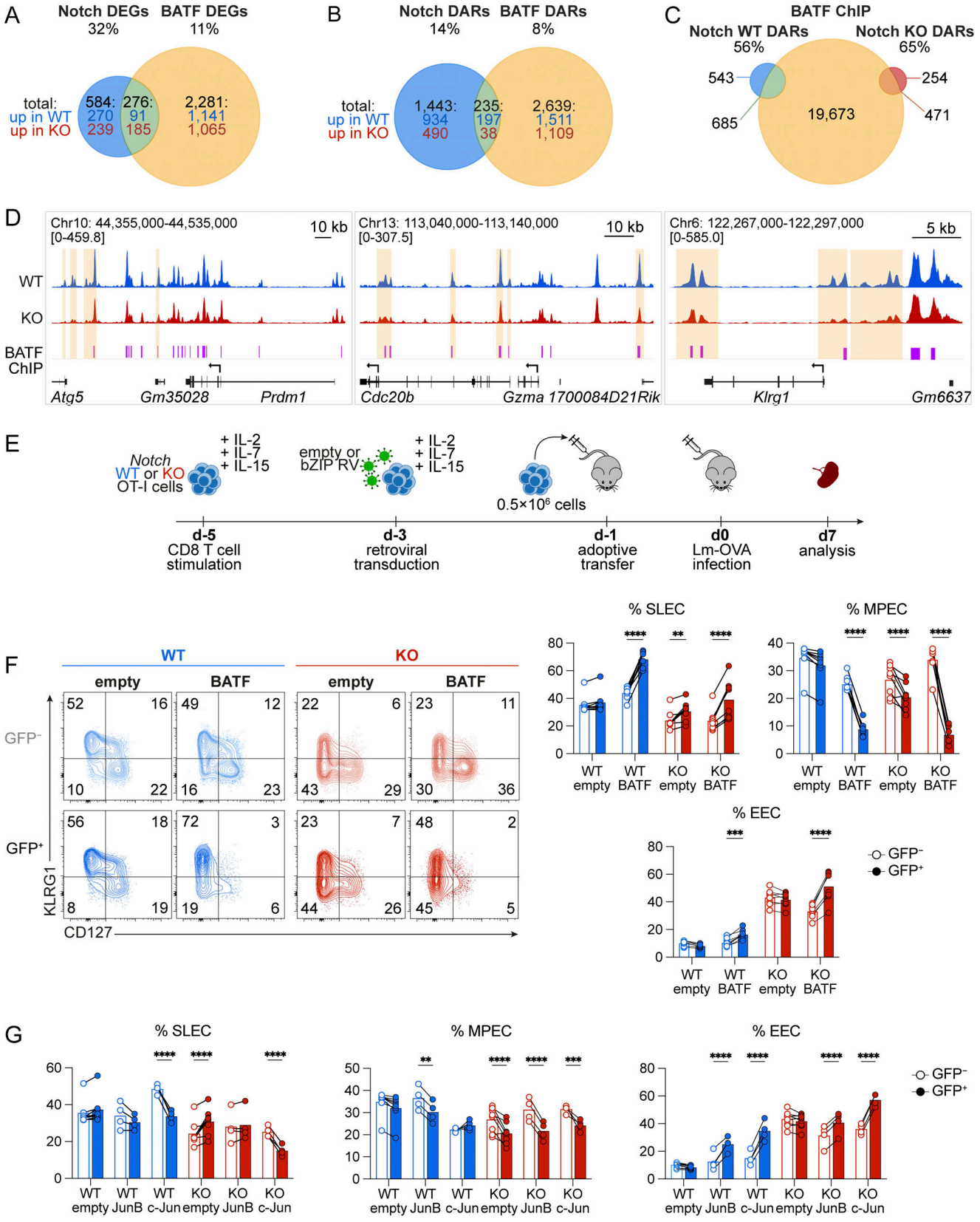

Figure 7. **Notch signaling promotes enhanced BATF activity to induce SLEC differentiation. (A)** Overlap between DEGs from available WT versus BATF cKO (Tsao et al., 2022) and WT versus Notch1/2 cKO (this paper) CD8⁺ T cells were determined while conserving the directionality of the data. **(B)** Overlap between Notch DARs (this paper) and BATF DARs (Tsao et al., 2022). **(C)** Overlap between Notch DARs (this paper) and available BATF binding sites obtained by chromatin immunoprecipitation with sequencing (ChIP-seq) (Tsao et al., 2022) is shown. **(D)** Notch WT or KO ATAC-seq tracks of genes important for CD8⁺

T cell effector differentiation or function are represented. DARs are highlighted in yellow, and BATF ChIP-seq peaks identified by Tsao et al. (2022) were also represented. **(E)** Naïve OT-I cells were stimulated with IL-7, IL-15, and IL-2 before transduction with an empty or bZIP-encoding defective retrovirus. Cells were adoptively transferred 2 days later, and mice were subsequently infected with Lm-OVA. On day (d) 7 after infection, spleens were collected for analysis. A fluorescent reporter (GFP) was used to trace cells that were successfully transduced. **(F)** Representative SLEC/MPEC plots gated on the transferred OT-I cells overexpressing BATF and compilation of SLEC, MPEC, and early effector cell (EEC) proportions. **(G)** Naïve OT-I cells were transduced with JUNB or c-JUN as in E. Compilation of SLEC, MPEC, and EEC proportions gated on OT-I CD8$^+$ T cells. Data are from one (G) or two (F) independent experiments with a total of n = 4–8 mice per group. Repeated measures two-way ANOVA with Sidak's multiple comparison test was used for GFP$^-$ versus GFP$^+$ comparisons. **P < 0.01, ***P < 0.001, ****P < 0.0001.

signals provided by FRCs is the activation of Notch signaling in CD8$^+$ T cells, which allows for the opening of chromatin regions controlling SLEC differentiation.

The presentation of Notch ligands within FRC niches is reminiscent of how Notch ligands govern pathogenic CD4$^+$ and CD8$^+$ T cell responses during GVHD, as well as the differentiation of Tfh cells (Fasnacht et al., 2014; Chung et al., 2017). Other studies reported an influence of Notch ligand expression by DCs on the differentiation of peripheral T cells (Backer et al., 2014; Maekawa et al., 2008; Sugimoto et al., 2010; Laky et al., 2015; Ito et al., 2009). Most of these studies were performed in vitro or used DCs artificially overexpressing Notch ligands aside from Laky et al. who showed that in vivo deletion of *Dll4* in DCs affects tumor control by CD4$^+$ T cells (Laky et al., 2015). Therefore, while DCs can provide Notch signals to T cells in certain contexts, FRCs emerge as the favored source of Notch ligands for activated T cells in multiple immune responses. This critical role of FRC Notch ligands could be related to early T cell positioning in FRC niches, prolonged FRC–T cell interactions, or temporal alignment of ligand–receptor pair expression.

Given the critical role of DLL Notch ligands in shaping the differentiation and homeostasis of other immune cells, such as MZB and ESAM^{hi} DCs (Fasnacht et al., 2014; Lewis et al., 2011; Skokos and Nussenzweig, 2007), our observations could result

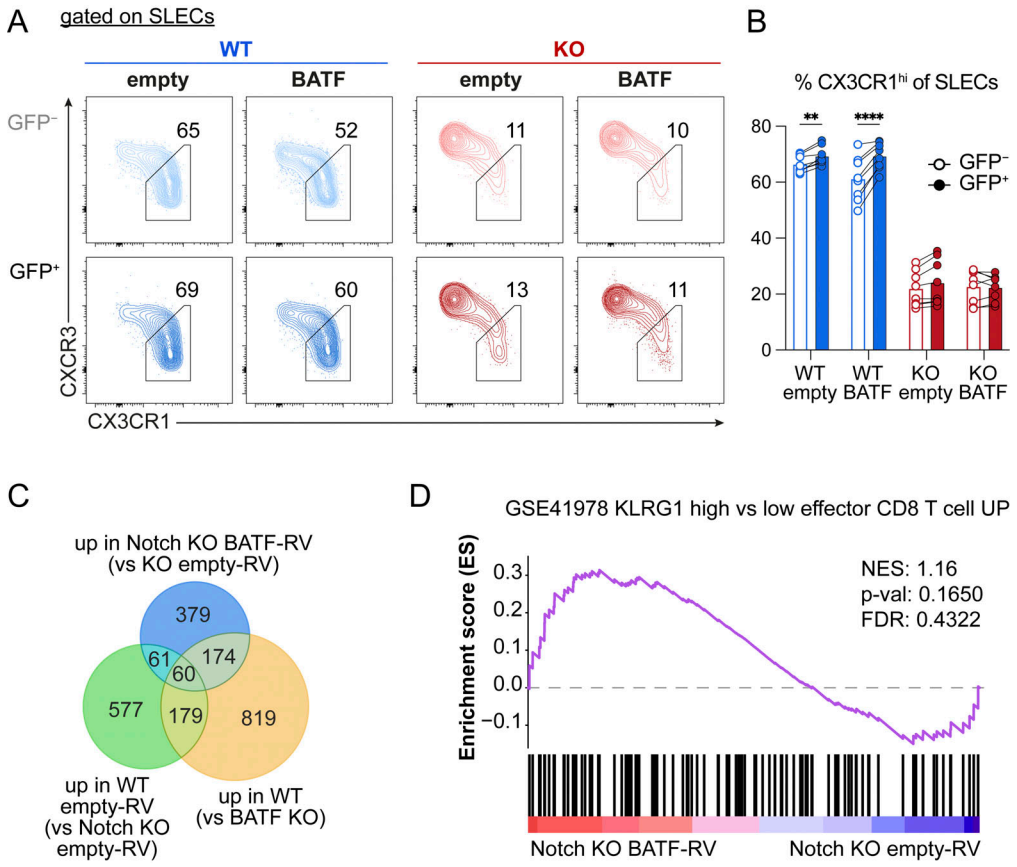

Figure 8. **BATF overexpression does not fully rescue the SLEC differentiation transcriptional program without Notch signaling. (A)** Differentiation of BATF overexpressing OT-I cells into CX3CR1^{hi}CXCR3^{lo} SLECs. BATF overexpression and OT-I T cell response were done as in Fig. 7. Representative CXCR3 versus CX3CR1 plots gated on OT-I SLECs. **(B)** Compilation of CX3CR1^{hi}CXCR3^{lo} SLECs as shown in A. **(C)** Venn diagram illustrating the overlap of the Notch (WT empty-RV versus Notch KO empty-RV), BATF (WT versus KO), and BATF overexpression in Notch KO (Notch KO BATF-RV versus Notch KO empty-RV). **(D)** BATF overexpression in Notch KO day 3 effector CD8$^+$ T cells does not lead to enrichment of the SLEC signature. NES, normalized enrichment score; FDR, false discovery rate. Data are from two independent experiments (A and B) with a total of n = 8 mice per group. Repeated measures two-way ANOVA with Sidak's multiple comparison test was used for GFP$^-$ versus GFP$^+$ comparisons. **P < 0.01, ****P < 0.0001.

from an indirect effect of stromal DLL1 and DLL4 on SLEC differentiation involving other cell types. This is unlikely for several reasons. First, anti-DLL1 blocking antibodies alone profoundly reduce MZB numbers (Tran et al., 2013), but fail to impact SLEC generation. Second, the loss of DLL1 and DLL4 in FRCs does not perturb the architecture of secondary lymphoid organs (Fasnacht et al., 2014; Chung et al., 2017). Third, *Dll1* and *Dll4* inactivation in FRCs does not affect overall CD8$^+$ T cell expansion following infection, arguing against the possibility that a DC defect underlies decreased SLEC differentiation. Finally, vaccination with in vitro matured BMDCs excludes any indirect effect of DLL1 and DLL4 loss on DC maturation in vivo.

ATAC-seq analysis showed that in Notch-sufficient cells, DARs with increased accessibility were associated with an effector signature, while those with decreased accessibility were linked to genes expressed in naïve T cells. Notch activation thus potentially operates as an epigenetic activator, promoting upregulated expression of genes crucial for effector differentiation, while being associated with repression of the naïve T cell state. Chromatin remodeling upon Notch activation could operate via recruitment of histone acetylases (e.g., p300) or chromatin remodeling complexes following NICD binding with RBPJ, as previously demonstrated (Kadam and Emerson, 2003; Takeuchi et al., 2007; Ntziachristos et al., 2012; Yatim et al., 2012; Wang et al., 2014, 2015; Schwanbeck, 2015; Skalska et al., 2015; Pillidge and Bray, 2019; Martin et al., 2023). H3K27 acetylation correlates with transcriptional activation, and dynamic binding of NOTCH1 increases H3K27Ac marks at enhancers in T cell acute lymphoblastic leukemias (Wang et al., 2014). This is in line with our findings, as a majority of DARs affected by Notch deficiency are distant from TSS, consistent with gene regulation by Notch via enhancers. The recent identification of interactions between ARID1A, a subunit of the cBAF chromatin remodeling complex, and NICD (Martin et al., 2023) suggests that the recruitment of ARID1A by NICD might help to open chromatin regions necessary for SLEC differentiation. It is therefore interesting to note that ARID1A deficiency affects effector CD8$^+$ T cell differentiation with a severe loss of CX3CR1$^+$ SLECs (McDonald et al., 2023).

Previous work showed enrichment of bZIP motifs within DARs defining effector/SLEC populations (Scott-Browne et al., 2016). The bZIP family includes members with similar DNA binding motifs but distinct functional roles. For example, AP-1 is required to open chromatin during T cell activation (Yukawa et al., 2020), while BACH2 is known to promote MPEC and memory differentiation (Roychoudhuri et al., 2016). Our results further demonstrate the differential effects of bZIP members on CD8$^+$ T cell response as only BATF, but not c-JUN or JUNB expression, promoted SLEC differentiation. BATF overexpression could not fully rescue Notch-driven SLEC differentiation as it failed to generate CX3CR1^{hi} SLECs. This suggests that Notch activation may render specific BATF binding sites accessible or that concerted action of NICD and BATF is required to drive expression of key SLEC-related genes. Alternatively, the differentiation of CX3CR1^{hi} SLECs might solely depend on Notch transcriptional activity or could require collaboration with other bZIPs. Recent studies reported that BATF is required to coordinate the binding of several key transcription factors to DNA, namely T-BET, JUND, IRF4, and STAT5 in CD8$^+$ T cells (Tsao et al., 2022). Thus, Notch activation may be associated with chromatin opening at specific regions to allow BATF-mediated transcription of pro-SLEC genes or support the function of other transcription factors, such as T-BET and STAT5 (Joshi et al., 2007). Interestingly, BATF acts early during CD8$^+$ T cell responses, further supporting the idea that it cooperates with Notch to regulate SLEC differentiation (Tsao et al., 2022). This would be consistent with the overlap of transcriptomes controlled by Notch and BATF (32%), as well as the enrichment of BATF binding sites in the DARs opened by Notch, notably at pro-effector loci (*Prdm1*, *Gzma*, and *Klrg1*) (Tsao et al., 2022). However, BATF overexpression in Notch-deficient CD8$^+$ T cells did not fully restore transcripts whose abundance was affected both by Notch and BATF deficiency. The exact mechanism of Notch and BATF target co-regulation remains unknown. One possibility is that the binding of NICD-RBPJ-BATF occurs in the same DNA regions, but we could not exclude long-range effects via chromatin remodeling and looping, or indirect effects. It would be interesting to investigate whether the recruitment of the cBAF complex via NICD-ARID1A is involved (Martin et al., 2023) as 50% of our Notch DARs have been shown to be bound by ARID1A in effector CD8$^+$ T cells (McDonald et al., 2023). Furthermore, ARID1A was shown to be necessary for BATF binding to DNA in effector CD8$^+$ T cells (McDonald et al., 2023) raising the possibility that NICD-ARID1A interactions are necessary to open chromatin regions where BATF binds during CD8$^+$ T cell differentiation.

Our work has allowed us to define the transcriptional outcome of Notch signaling in T cells, revealing a T cell–specific Notch signature that will be useful to probe for Notch signaling in T cells in different contexts. This is highlighted by the ability of this novel signature to detect Notch signaling in human T cells during multi-inflammatory syndrome in children infected with SARS-CoV-2.

In conclusion, our results reveal an essential role for DLL1 and DLL4 expression by secondary lymphoid organ FRCs in SLEC differentiation. The early Notch signals provided by these specialized stromal cell niches ultimately control a T cell–specific epigenetic and transcriptional signature that correlates with open effector-associated chromatin regions and enhanced BATF activity to promote the SLEC differentiation program.

Materials and methods

Mice

B6-CD45.1, C57BL/6, and OT-I *Rag1*–deficient (Hogquist et al., 1994) mice were bred at the Maisonneuve-Rosemont Hospital Research Center or Institut de recherches cliniques de Montréal animal facilities. *Notch1*$^{fl/fl}$ (*N1*$^{fl/fl}$), E8I-Cre$^{-\text{ or }+}$ × *N1*$^{fl/fl}$ (*Notch1* WT or KO), *Notch2*$^{fl/fl}$ (*N2*$^{fl/fl}$), *E8I*-Cre$^{-\text{ or }+}$ × *N2*$^{fl/fl}$ (*Notch2* WT or KO), E8I-Cre$^{-\text{ or }+}$ × *N1*$^{fl/fl}$*N2*$^{fl/fl}$ (*Notch1/2* WT or KO), and E8I-Cre$^{-\text{ or }+}$ × *N1*$^{fl/fl}$*N2*$^{fl/fl}$ OT-I *Rag1*$^{-/-}$ (*Notch1/2* WT or KO OT-I) were bred as described (Mathieu et al., 2015). All mice were bred and housed in a pathogen-free environment and treated in accordance with the Canadian Council on Animal Care guidelines.

Our protocol was approved by the Hospital Maisonneuve–Rosemont and Institut de recherches cliniques de Montréal Committee on Animal Care. *Dll1*$^{fl/fl}$, *Dll4*$^{fl/fl}$, Ccl19-Cre$^{-\text{ or }+}$ × *Dll1*$^{fl/fl}$*Dll4*$^{fl/fl}$ (stromal fl/fl or Δ/Δ), Mx-Cre$^{-\text{ or }+}$ × *Dll1*$^{fl/fl}$*Dll4*$^{fl/fl}$ (DC fl/fl or Δ/Δ) CD4-Cre X *ROSAdnMAMLf* mice were previously described in Zhang et al. (2011), Chung et al. (2017), and were bred at the University of Michigan or the University of Pennsylvania or Institut de recherches cliniques de Montréal. The animal protocol for these mice was approved by the University of Michigan's Committee on Use and Care of Animals or the University of Pennsylvania's Office of Regulatory Affairs and the Institut de recherches cliniques de Montréal Committee on Animal Care.

Analysis of CD8$^+$ T cell response

To induce a CD8$^+$ T cell response, mice were either injected i.v. with 2 × 10^3 CFU of Lm-OVA as previously described (Bahjat et al., 2006) or immunized with BMDCs loaded with the $OVA_{257-264}$ peptide (SIINFEKL; Sigma-Aldrich). GM-CSF + IL-4 and FLT3L BMDCs were generated as previously described (Boulet et al., 2019). On the eve of the last day of culture, BMDCs were matured with LPS alone (GM-CSF + IL4 BMDCs, 100 ng/ml; Sigma-Aldrich) or with LPS and the TLR7/8 agonist R848 (FLT3L BMDCs, 100 ng/ml; Sigma-Aldrich), as previously described, and then loaded with OVA peptide (2 µg/ml; Sigma-Aldrich). A total of 5 × 10^5 DCs were i.v. injected. In experiments with adoptive transfers of OT-I T cells, 10^6 or 10^4 cells were transferred into recipient mice 1 day prior to Lm-OVA infection. Mice that received 10^6 OT-I T cells were sacrificed on day 2 or 3 after infection, while mice that received 10^4 OT-I T cells were sacrificed either on day 5 or 7 after infection. Ex vivo CD8$^+$ T cell responses were analyzed in the spleen.

In selected experiments, recipient mice received humanized IgG1 monoclonal antibodies (mAbs) specific for DLL1 or DLL4 (Genentech, Inc.) or a combination of both mAbs (5 mg/kg i.p.) (Ridgway et al., 2006; Tran et al., 2013). In these experiments, anti-HSV gD human IgG1 (Genentech, Inc.) was used as an isotype control antibody.

Recall response of memory CD8$^+$ T cells

B6-CD45.1 mice were adoptively transferred with 10^4 WT or *Notch1/2* KO OT-I cells (CD45.2$^+$) and infected with Lm-OVA as described above. On day 30 after infection, mice were rechallenged with 1 × 10^4 CFU of Lm-OVA, and 5 days after rechallenge, the CD8$^+$ T cell response (CD8$^+$CD45.2$^+$) was assessed among splenocytes. Mice adoptively transferred with WT OT-I cells received DLL1 and DLL4-specific mAbs on the day of the rechallenge and 2 days later.

Adoptive transfer of WT or *Notch1/2* KO CD25^{hi} OT-I cells

B6-CD45.1 mice were adoptively transferred with OT-I cells and infected with Lm-OVA as described above. 72 h after infection, splenocytes were purified by negative selection using anti-CD4 and anti-CD19 biotinylated antibodies and streptavidin-conjugated magnetic beads (EasySep Streptavidin RapidSpheres from StemCell). CD25^{hi} OT-I cells (Zombie dye$^-$ CD8$^+$ CD45.2$^+$ CD44$^+$ CD25^{hi}) were then sorted and 5 × 10^4 were transferred into match-infected B6-CD45.1 mice. On day 7 after infection, the CD8$^+$ T cell response was assessed among splenocytes.

Retroviral (RV) transduction

MSCV-*Batf*-IRES-eGFP, MSCV-*JunB*-IRES-eGFP, and MSCV-*cJun*-IRES-eGFP plasmids were kindly gifted by Patrick G. Hogan (La Jolla Institute for Immunology, San Diego, CA, USA). RV particles were produced by transfection of 293T cells with MSCV and pCL-Eco plasmids using Lipofectamine 2000 and RVs were collected on days 2 and 3 after transfection.

For RV transduction, E8I-Cre$^{-\text{ or }+}$ × *Notch1/2*$^{fl/fl}$ OT-I cells (CD45.2$^+$) were isolated from lymph nodes, resuspended to a final concentration of 2 × 10^6 cells/ml in complete RPMI medium (Nu-Serum 10%, Penicillin-Streptomycin 100 U/ml, L-glutamine 2 mM, β-mercaptoethanol 50 µM, non-essential amino acid 0.1 mM, sodium pyruvate 1 mM, HEPES 10 mM) supplemented with IL-7 (25 ng/ml), IL-15 (100 ng/ml), and IL-2 (20 ng/ml) to induce homeostatic proliferation. After 48 h in culture, cells were spin-transduced with RV supernatant in the presence of polybrene (8 µg/ml) at 2,500 rpm for 1 h at 37°C. Cells were then incubated for an additional 2–4 h at 37°C before being resuspended to a final concentration of 2 × 10^6 cells/ml in RPMIc supplemented with IL-7 (25 ng/ml), IL-15 (100 ng/ml), and IL-2 (20 ng/ml) (Connolly et al., 2021). Transduced OT-I cells were transferred (0.5 × 10^6) into B6-CD45.1 mice (CD45.1$^+$) 48 h later to ensure optimal bZIP overexpression. Lm-OVA infection was performed the following day, and CD8$^+$ T cell response was measured 7 days after infection.

Flow cytometry and cell sorting

Spleens and lymph nodes were dissociated using frosted glass slides. Red blood cell lysis was performed on spleens using 0.83% NH_4Cl for 5 min at room temperature. Tetramer H2-K^b-$OVA_{257-264}$ (obtained from the National Institutes of Health Tetramer Core Facility) staining was performed at 37°C for 15 min. Extracellular staining was performed for 20 min at 4°C in FACS wash buffer, as previously described (Ostiguy et al., 2007). A complete list of antibodies used in this article is available in Table S4.

For kinetic analysis of Notch2 expression, splenocytes were stained with a Zombie dye following the manufacturer's protocol (Biolegend). Extracellular staining was performed for 20 min at 4°C in FACS wash buffer, as previously described. Then, cells were fixed and permeabilized using the eBioscience Foxp3 staining buffer following the manufacturer's protocol. Intracellular staining with uncoupled anti-Notch2 antibody (Cell Signaling) was then performed in permeabilization buffer for 30 min at 4°C. Finally, a goat anti-rabbit IgG (H+L) highly cross-adsorbed secondary antibody (Invitrogen) was used to target uncoupled Notch2 in the permeabilization buffer for 15 min at 4°C.

For analysis of p-STAT5a, p-STAT4, and p-STAT3a, splenocytes were rested 2 h in RPMI and then stimulated for 30 min in complete RPMI (10% FBS) with IL-2 (100 U/ml), IL-15 (20 ng/ml), IL-12 (20 ng/ml), or IL-21 (20 ng/ml). Following stimulation, cells were stained with a Zombie dye following the manufacturer's

protocol (Biolegend). Cells were then fixed with PFA 1% at room temperature for 15 min and permeabilized with 100% ice-cold methanol at −20°C for 20 min. Finally, extra and intracellular staining was done simultaneously in PBS/FBS 1% buffer at room temperature for 30 min. Flow cytometry analysis was performed on a BD LSR II or BD LSRFortessa X-20 from BD Biosciences and data were analyzed using FlowJo software (Tree Star).

For the analysis of cytokine production, day 7 ex vivo splenocytes were collected and stimulated with the OVA peptide (2 µg/ml) in the presence of brefeldin A (10 µg/ml) for 5 h at 37°C. Briefly, restimulated cells were fixed for 20 min with 1% paraformaldehyde at room temperature. Fixed cells were permeabilized with saponin (0.5%) in FACS wash buffer for 10 min at room temperature (RT) and stained with anti-cytokine or anti-granzyme B antibodies followed by cell surface staining.

For cell sorting, cell suspensions were incubated with a viability dye and Fc-block (αCD16/32; BioXcell) for 10 min at RT and then stained with extracellular antibodies for 20 min at 4°C in sorting buffer (PBS, 1% Nu serum [Corning], 1 mM EDTA, and 25 mM HEPES). Cells were sorted with a BD FACSAria III.

For RNA-seq of WT versus *Notch1/2* KO OT-I cells, naïve OT-I cells (Zombie dye$^-$ CD8$^+$ CD45.2$^+$ CD25$^-$ CD69$^-$ CD44$^-$) from pooled lymph nodes and spleens and activated OT-I cells (Zombie dye$^-$ CD8$^+$ CD45.2$^+$ CD44$^+$) from spleens were sorted on day 3 after infection. For naïve cells, a total of three individual biological samples from three independent experiments were collected for each genotype (6×10^5–3×10^6 cells/sample). For activated cells, a total of eight individual biological samples from three independent experiments were collected for each genotype (1.9×10^4–1.1×10^5 cells/sample).

For RNA-seq of WT versus *Notch1/2* KO OT-I cells transduced with empty-RV or BATF-RV as described above, transduced OT-I cells (Zombie dye$^-$ CD8$^+$ CD45.2$^+$ CD44$^+$ GFP$^+$) were isolated from spleens on day 3 after infection. A total of four individual biological samples from one independent experiment were collected for each condition (6×10^4–1×10^5 cells/sample).

RNA-seq sample preparation

Cells were FACS-sorted directly into TRIzol reagent and frozen at −80°C. RNA extraction, library preparation, and sequencing were done at the IRIC Genomics Platform (University of Montreal). For cDNA library preparation, 150 ng RNA was used, and cDNA library sequencing was performed on Illumina Nextseq500 (75 cycles of single-end reads).

RNA-seq analysis

For experiments comparing the transcriptomes of *Notch1/2* WT and KO CD8$^+$ T cells and OT-I in vitro activated T cells culture on OP9 versus OP9-DLL4 (Mohtashami et al., 2010), bioinformatics analysis was done at the IRIC Genomics Platform and at the Institut de recherches cliniques de Montréal (IRCM). Sequenced reads were trimmed for sequencing adapters and low-quality 3′ bases using Trimmomatic version 0.35 (Bolger et al., 2014) and then aligned to the reference mouse genome version GRCm38 (or mm10 gene annotation from Gencode version M13, based on Ensembl 88) using STAR version 2.5.1b (Dobin et al., 2013). Gene expression was obtained both as read count directly from STAR as well as computed using RSEM (Li and Dewey, 2011) to obtain gene and transcript level expression, either in transcripts per kilobase million or fragments per kilobase per million mapped reads values for these stranded RNA libraries. DESeq2 version 1.16.1 was then used to normalize gene read counts and compute differential expression between different experimental conditions (Love et al., 2014).

GO term enrichment analysis of differentially expressed genes was performed using DAVID (Huang et al., 2009) and the determination of relevant upstream regulators was done with QIAGEN's IPA. GSEA enrichment analysis was performed using the Broad Institute's software and MSigDB (https://www.gsea-msigdb.org/gsea/index.jsp) (Subramanian et al., 2005).

For experiments evaluating the impact of BATF overexpression, sequences were trimmed with Trimmomatic version 0.39 (Bolger et al., 2014) and aligned to reference genome GRCm38 using STAR version 2.7.8a (Dobin et al., 2013). Gene counts were determined with featureCounts (Liao et al., 2014). Robust principal component analysis (Chen et al., 2020) was used to detect outlier samples, and two samples (one KO-empty and one KO-BATF sample) were therefore excluded from differential expression analysis. DESeq2 v1.24.0 was used to determine differential expression (Love et al., 2014).

Quantitative real-time PCR

Total RNA was isolated from cells sorted in TRIzol, followed by reverse transcription into cDNA using SuperScript II and oligo(dT) primers (Invitrogen). Subsequently, the quantitative PCR (qPCR) reaction was performed using Power SYBR Green (Applied Biosystems) on a 7500 Real-Time PCR System (Applied Biosystems). Each sample was normalized to the endogenous reference gene *Hprt* and to a reference sample (calibrator), as previously described (Boulet et al., 2014). The differential cycle threshold (ΔC_T) value for each sample was determined by calculating the CT value difference between the target gene and *Hprt*. Next, the $\Delta\Delta C_T$ was computed for each sample by subtracting the mean ΔC_T of the sample from the ΔC_T of the calibrator. The relative expression of the target gene was calculated using $2^{-\Delta\Delta C_T}$. Primer sequences are as follows: *Hprt*, 5′-CTCCTC AGACCGCTTTTTGC-3′ and 5′-TAACCTGGTTCATCATCGCTA ATC-3′; *Dll1*, 5′-GGATACACACAGCAAACGTGA-3′ and 5′-CGC TTCCATCTTACACCTCAG-3′; *Dll4*, 5′-GGAACCTTCTCACTCAAC ATCC-3′ and 5′-CTCGTCTGTTCGCCAAATCT-3′.

T cell Notch signature

RNA-seq data from this paper and Chung et al. were reanalyzed with the same pipeline (Chung et al., 2019). Briefly, the first 10 base pairs from sequence reads were trimmed with Trimmomatic version 0.36 (Bolger et al., 2014) and aligned to reference genome GRCm38 using STAR version 2.5.1b (Dobin et al., 2013). Gene counts were determined with featureCounts (Liao et al., 2014). DESeq2 v1.24.0 was used to determine differential expression (Love et al., 2014). DEGs with an adjusted P value <0.05 were kept for further analysis. This included 875 DEGs for CD8$^+$ T cells and 622 DEGs for CD4$^+$ T cells. 136 DEGs were similarly regulated in the CD4$^+$ and CD8$^+$ T cells datasets; 82 genes were

upregulated and 54 downregulated in the absence of Notch signaling. These 136 genes were thus defined as the Notch T cell signature (Table S2).

Enrichment of the Notch T cell signature was tested in publicly available mouse (GSE131847) and human (Benamar et al., 2023) scRNA-seq data. The FeaturePlot_scCustom() function from the scCustomize package in R was used to score the Notch signature gene sets on murine and human data. Mouse data from GSE131847 were imported and analyzed using Seurat. Doublets or dead cells were filtered out and downstream analysis was performed using default values. Human data from healthy and COVID MIS-C patients were reanalyzed. The Cellranger (7.0.1) multi pipeline was used to analyze 10 × 3′ Cell Multiplexing data from different patients. The resulting gene expression matrices for each sample were then imported into the R package Seurat for quality control and downstream analyses (Satija et al., 2015). For each sample, empty/dead cells or doublets were filtered out based on the number of transcripts, number of unique genes present, and percentage of mitochondrial reads. Samples were then normalized and highly variable genes were identified prior to integration. Linear dimensionality reduction was performed by principal component (PC) analysis. Only the first 15 PCs were selected for subsequent analyses. Clusters were identified using Louvain's algorithm with a resolution of 0.5. The resulting clusters were automatically labeled using the fine labels from the MonacoImmune reference dataset from the celldex library. Cells labeled as CD4 were subsetted and reanalyzed (15 dimensions, resolution 0.5). Uniform Manifold Approximation and Projection (UMAP) was applied for visualization purposes.

ATAC-seq sample preparation

B6-CD45.1 mice were adoptively transferred with WT versus *Notch1/2* KO OT-I cells and infected with Lm-OVA as described above. 72 h after infection, splenocytes were purified by negative selection using anti-CD4 and anti-CD19 biotinylated antibodies and streptavidin-conjugated magnetic beads (EasySep Streptavidin RapidSpheres, StemCell Technologies). Activated OT-I cells (Zombie dye$^-$ CD8$^+$ CD45.2$^+$CD44$^+$) were then sorted and nuclei isolation was performed as previously described (Odagiu et al., 2020). Briefly, cells were kept on ice, washed twice in ice-cold PBS without Ca^{2+}/Mg^{2+}, and centrifuged for 5 min at 1,300 rpm. Cells were resuspended in one volume of ice-cold PBS before adding four volumes of lysis buffer (12.5 mM Tris, pH 7.4; 45 mM KCl; 6.25 mM $MgCl_2$; 375 mM sucrose; 0.125% Nonidet P-40; 1 tablet of complete [EDTA free] protease inhibitor mixture [Roche]/50 ml). After 10 min of incubation on ice, lysed cells were centrifuged at 4°C for 7 min at 500 *g*. The nuclei pellet was resuspended in a tenth of the original lysis volume in wash buffer (10 mM Tris, pH 7.4; 60 mM KCl; 15 mM NaCl; 5 mM $MgCl_2$; 300 mM sucrose). Then, wash buffer was added to half of the lysis volume, and nuclei were centrifuged at 4°C for 7 min at 500 *g*. Washed nuclei were counted and 50,000 nuclei were used for the transposase reaction. ATAC-seq was performed as previously described (Odagiu et al., 2020) with some modifications (Tn5 tagmentation, DNA purification, and library preparation were performed at the Montreal Clinical Research Institute Genomics Platform; sequencing was performed by the Centre d'expertise et de services of Génome Québec). Briefly, 5 × 10^4 nuclei were directly treated with Tn5 transposase at 37°C for 30 min. After the enzymatic reaction, the DNA was purified by Mini-Elute PCR Purification columns (Qiagen) and enriched by 12 PCR cycles. The library was recovered from PCR by GeneRead Purification columns (Qiagen) and double-strand sequenced on Illumina NovaSeq 6000 S4 PE100. A total of 112 × 10^6–132 × 10^6 reads/samples were obtained. For footprinting analysis, libraries were resequenced to allow increased sequencing depth, and an additional 103 × 10^6–149 × 10^6 reads/sample were obtained.

ATAC-seq analysis

The quality of the raw reads was assessed with FASTQC v0.11.8. Trimming was then performed with TRIMMOMATIC v0.36 (Bolger et al., 2014). Reads were aligned to the mouse reference genome mm10 with BOWTIE2 v2.2.6 (Langmead and Salzberg, 2012) with a mean of 57% of reads uniquely mapped. Alignments were post-processed to remove PCR duplicates (Picard tool v2.4.1) and reads were mapped to mitochondrial DNA (samtools v1.8). To represent the real Tn5 transposase binding sites of 9 bp, the coordinates of the reads were shifted by 4 bp for the plus strand and by 5 bp for the minus strand using Deeptools v3.0.1 (Ramírez et al., 2016). The former was also used to remove ENCODE's blacklisted regions (signal artifact regions) and convert Bam files to BEDPE format. MACS2 was used to identify significant peaks (Zhang et al., 2008). Diffbind v2.10.0 R package was used to generate the count matrix of Tn5 insertion site numbers for each consensus peak (peaks that were present in all samples for each condition). DARs were identified between WT versus *Notch1/2* KO OT-I cells using DESeq2 v1.30.0 R package (Love et al., 2014). DARs were annotated with their closest feature and different transcription binding motifs identified with HOMER v4.8.0. An unbiased motif search was also performed with HOMER to identify all known motifs and de novo motifs in these regions.

Footprinting analysis was done with the HMM-based IdeNtification of Transcription factor footprints (HINT) library from the Regulatory Genomics Toolbox (RGT) software (version 0.13.2 [Li et al., 2019]). Footprints were called from chromatin-accessible regions (called by MACS2 2.6) for each sample and then matched to motifs using JASPAR 2020. Differential activity of transcription factors was assessed using HINT-differential, while P value and read counts were calculated using RGT HINT-differential.

Bioinformatics analysis was performed at the Bioinformatics core facility from IRCM.

Statistical analysis

Statistical analyses for differences between the fl/fl and Δ/Δ groups were done using a two-tailed Student's *t* test. Welch's correction was applied for unequal variances when required. Wilcoxon signed-rank test was used when comparing two groups with matched pairs. ANOVA analysis (Kruskal–Wallis test) with Dunn's multiple comparisons was used when comparing more than two experimental groups. Tukey's correction

was applied for unequal variances when required. Data are presented as mean ± standard error of the mean (SEM). Only significant statistical differences are indicated on the figures, and *P < 0.05, **P < 0.01, ***P < 0.001, ****P < 0.0001 were considered statistically significant.

Online supplemental material

Fig. S1 shows DLL1 and DLL4 expression in GM-CSF or FLT3L BMDCs and mRNA expression on cDC1 and cDC2, as well as cytokine production by OVA-specific CD8⁺ T cells following Lm-OVA infection. Fig. S2 shows SLEC differentiation of memory CD8⁺ T cells following rechallenge with Lm-OVA. Fig. S3 shows the impact of the timing of αDLL1/4 blockade on SLEC differentiation following Lm-OVA infection, as well as the recovery and viability of OT-I CD8⁺ T cells on day 3 after infection with Lm-OVA. Fig. S4 shows our Notch T cell signature applied to publicly available datasets of T cell transcriptomes during an immune response. Fig. S5 shows HOMER motif enrichment analysis and footprints of several bZIP transcription factors. Table S1 shows the 217 differentially expressed genes (Padj ≤0.05 and |fold change| >1.5) between *Notch1/2* WT and KO CD8+ T cells. Table S2 shows the 136 genes included in the T-cell Notch transcriptional signature. Table S3 shows the mROAST enrichment analysis results of the Notch T cell signature against other published datasets. Table S4 shows the complete list of antibodies used in this article.

Data availability

The raw sequencing data have been deposited in NCBI's Gene Expression Omnibus (GEO). RNA sequencing data underlying Fig. 3, E–G; Fig. 4; Fig. 5, A–C; Fig. 7 A; Fig. 8, C and D; Fig. S3 G; and Fig. S4 are accessible through GEO Series accession number GSE289394. ATAC sequencing data underlying Fig. 6; Fig. 7, B–D; and Fig. S5 are accessible through GEO Series accession number GSE289392.

Acknowledgments

We would like to acknowledge all lab members for helpful discussions, R. Hétu-Arbour for technical assistance, M. Dupuis and F. Duval for cell sorting, and animal care technicians for animal husbandry. We thank P. Hogan (La Jolla Institute for Immunology, La Jolla, CA, USA) for kindly providing the retroviral vector coding for BATF, JUNB, and c-JUN. We thank Juan-Carlos Zuniga-Pflücker (Immunology Department, University of Toronto, Toronto, Canada) for providing the OP9 and OP9-DLL4 cell lines. We thank É. Gagnon (Institute for Research in Immunology and Cancer, Université de Montréal, Montreal, Canada) for sharing the transduction protocol of naïve T cells. We are grateful to V. Calderon (Institut de Recherches Cliniques de Montréal, Montreal, Canada) and C. Grou (Institut de Recherches Cliniques de Montréal, Montreal, Canada) for bioinformatics analysis.

This work was supported by grants from the Canadian Institutes of Health Research (PJT-152988 and PJT-180326) to N. Labrecque and from the National Institute of Allergy and Infectious Diseases (NIAID; R01-AI091627) and National Cancer Institute (NCI; R01-CA278976) to I. Maillard. E. Perkey was supported by T32-GM007863 from the National Institute for General Medical Sciences and F30-AI136325 from NIAID. J.D. Brandstadter was supported by T32-HL07439 from the National Heart, Lung and Blood Institute and by a career development award from the American Society of Transplantation and Cellular Therapy. K. Lederer was supported by T32-AI055428 from NIAID. D. Maurice De Sousa and L. Le Corre were supported by a studentship from the Fonds de la Recherche Québec-Santé. F. Duval was supported by a studentship from the University of Montreal.

Author contributions: D. Maurice De Sousa: Conceptualization, Formal analysis, Investigation, Methodology, Project administration, Validation, Visualization, Writing - original draft, Writing - review & editing, E. Perkey: Formal analysis, Investigation, Methodology, Visualization, Writing - review & editing, L. Le Corre: Conceptualization, Data curation, Formal analysis, Investigation, Methodology, Project administration, Software, Validation, Visualization, Writing - original draft, Writing - review & editing, S. Boulet: Conceptualization, Data curation, Formal analysis, Investigation, Writing - original draft, D. Gómez Atria: Formal analysis, Investigation, A. Allman: Formal analysis, Investigation, F. Duval: Conceptualization, Formal analysis, Investigation, Methodology, J.-F. Daudelin: Conceptualization, Formal analysis, Funding acquisition, Investigation, Methodology, Project administration, Resources, Supervision, Validation, Writing - review & editing, J.D. Brandstadter: Conceptualization, K. Lederer: Data curation, S. Mezrag: Formal analysis, Investigation, Validation, L. Odagiu: Formal analysis, Investigation, Validation, M. Ennajimi: Investigation, M. Sarrias: Resources, H. Decaluwe: Resources, U. Koch: Resources, F. Radtke: Methodology, Resources, Writing - review & editing, B. Ludewig: Methodology, Resources, Writing - review & editing, C.W. Siebel: Resources, I. Maillard: Conceptualization, Funding acquisition, Methodology, Project administration, Resources, Supervision, Writing - original draft, Writing - review & editing, N. Labrecque: Conceptualization, Funding acquisition, Methodology, Project administration, Resources, Supervision, Validation, Visualization, Writing - original draft, Writing - review & editing.

Disclosures: D. Gómez Atria reported personal fees from Aro Biotherapeutics and GlaxoSmithKline outside the submitted work. J.D. Brandstadter reported personal fees from Recordati during the conduct of the study. C.W. Siebel reported personal fees from Genentech during the conduct of the study and personal fees from Genentech outside the submitted work. I. Maillard reported grants from NIAID and grants from NCI during the conduct of the study; "other" from Regeneron, Genentech, and Garuda Therapeutics; and grants from the Commonwealth of Pennsylvania outside the submitted work. N. Labrecque reported personal fees from *The Journal of Immunology* outside the submitted work. No other disclosures were reported.

Submitted: 27 September 2023
Revised: 6 September 2024
Accepted: 19 February 2025

References

Alexandre, Y.O., D. f, H.J. Lee, L.C. Gandolfo, C.G. Williams, S. Devi, B. Pal, J.R. Groom, W. Cao, S.N. Christo, et al. 2022. A diverse fibroblastic stromal cell landscape in the spleen directs tissue homeostasis and immunity. *Sci. Immunol.* 7:eabj0641. https://doi.org/10.1126/sciimmunol.abj0641

Amsen, D., J.M. Blander, G.R. Lee, K. Tanigaki, T. Honjo, and R.A. Flavell. 2004. Instruction of distinct CD4 T helper cell fates by different notch ligands on antigen-presenting cells. *Cell.* 117:515–526. https://doi.org/10.1016/s0092-8674(04)00451-9

Amsen, D., C. Helbig, and R.A. Backer. 2015. Notch in T cell differentiation: All things considered. *Trends Immunol.* 36:802–814. https://doi.org/10.1016/j.it.2015.10.007

Araki, K., A.P. Turner, V.O. Shaffer, S. Gangappa, S.A. Keller, M.F. Bachmann, C.P. Larsen, and R. Ahmed. 2009. mTOR regulates memory CD8 T-cell differentiation. *Nature*. 460:108–112. https://doi.org/10.1038/nature08155

Backer, R.A., C. Helbig, R. Gentek, A. Kent, B.J. Laidlaw, C.X. Dominguez, Y.S. de Souza, S.E. van Trierum, R. van Beek, G.F. Rimmelzwaan, et al. 2014. A central role for Notch in effector CD8(+) T cell differentiation. *Nat. Immunol.* 15:1143–1151. https://doi.org/10.1038/ni.3027

Badovinac, V.P., K.A.N. Messingham, A. Jabbari, J.S. Haring, and J.T. Harty. 2005. Accelerated CD8$^+$ T-cell memory and prime-boost response after dendritic-cell vaccination. *Nat. Med.* 11:748–756. https://doi.org/10.1038/nm1257

Bahjat, K.S., W. Liu, E.E. Lemmens, S.P. Schoenberger, D.A. Portnoy, T.W. Dubensky Jr., and D.G. Brockstedt. 2006. Cytosolic entry controls CD8$^+$-T-cell potency during bacterial infection. *Infect. Immun.* 74:6387–6397. https://doi.org/10.1128/iai.01088-06

Bellomo, A., I. Mondor, L. Spinelli, M. Lagueyrie, B.J. Stewart, N. Brouilly, B. Malissen, M.R. Clatworthy, and M. Bajénoff. 2020. Reticular fibroblasts expressing the transcription factor WT1 define a stromal niche that maintains and replenishes splenic red pulp macrophages. *Immunity*. 53:127–142.e7. https://doi.org/10.1016/j.immuni.2020.06.008

Benamar, M., Q. Chen, J. Chou, A.M. Julé, R. Boudra, P. Contini, E. Crestani, P.S. Lai, M. Wang, J. Fong, et al. 2023. The Notch1/CD22 signaling axis disrupts Treg function in SARS-CoV-2-associated multisystem inflammatory syndrome in children. *J. Clin. Invest.* 133:e163235. https://doi.org/10.1172/jci163235

Bolger, A.M., M. Lohse, and B. Usadel. 2014. Trimmomatic: A flexible trimmer for Illumina sequence data. *Bioinformatics*. 30:2114–2120. https://doi.org/10.1093/bioinformatics/btu170

Boulet, S., J.-F. Daudelin, and N. Labrecque. 2014. IL-2 induction of Blimp-1 is a key in vivo signal for CD8$^+$ short-lived effector T cell differentiation. *J. Immunol.* 193:1847–1854. https://doi.org/10.4049/jimmunol.1302365

Boulet, S., J.-F. Daudelin, L. Odagiu, A.-N. Pelletier, T.J. Yun, S. Lesage, C. Cheong, and N. Labrecque. 2019. The orphan nuclear receptor NR4A3 controls the differentiation of monocyte-derived dendritic cells following microbial stimulation. *Proc. Natl. Acad. Sci. USA*. 116:15150–15159. https://doi.org/10.1073/pnas.1821296116

Brown, F.D., D.R. Sen, M.W. LaFleur, J. Godec, V. Lukacs-Kornek, F.A. Schildberg, H.-J. Kim, K.B. Yates, S.J.H. Ricoult, K. Bi, et al. 2019. Fibroblastic reticular cells enhance T cell metabolism and survival via epigenetic remodeling. *Nat. Immunol.* 20:1668–1680. https://doi.org/10.1038/s41590-019-0515-x

Camara, A., O.G. Cordeiro, F. Alloush, J. Sponsel, M. Chypre, L. Onder, K. Asano, M. Tanaka, H. Yagita, B. Ludewig, et al. 2019. Lymph node mesenchymal and endothelial stromal cells cooperate via the RANK-RANKL cytokine axis to shape the sinusoidal macrophage niche. *Immunity*. 50:1467–1481.e6. https://doi.org/10.1016/j.immuni.2019.05.008

Chai, Q., L. Onder, E. Scandella, C. Gil-Cruz, C. Perez-Shibayama, J. Cupovic, R. Danuser, T. Sparwasser, S.A. Luther, V. Thiel, et al. 2013. Maturation of lymph node fibroblastic reticular cells from myofibroblastic precursors is critical for antiviral immunity. *Immunity*. 38:1013–1024. https://doi.org/10.1016/j.immuni.2013.03.012

Charbonnier, L.-M., S. Wang, P. Georgiev, E. Sefik, and T.A. Chatila. 2015. Control of peripheral tolerance by regulatory T cell-intrinsic Notch signaling. *Nat. Immunol.* 16:1162–1173. https://doi.org/10.1038/ni.3288

Chen, J., I.F. López-Moyado, H. Seo, C.J. Lio, L.J. Hempleman, T. Sekiya, A. Yoshimura, J.P. Scott-Browne, and A. Rao. 2019. NR4A transcription factors limit CAR T cell function in solid tumours. *Nature*. 567:530–534. https://doi.org/10.1038/s41586-019-0985-x

Chen, X., B. Zhang, T. Wang, A. Bonni, and G. Zhao. 2020. Robust principal component analysis for accurate outlier sample detection in RNA-Seq data. *BMC Bioinformatics*. 21:269. https://doi.org/10.1186/s12859-020-03608-0

Chung, J., C.L. Ebens, E. Perkey, V. Radojcic, U. Koch, L. Scarpellino, A. Tong, F. Allen, S. Wood, J. Feng, et al. 2017. Fibroblastic niches prime T cell alloimmunity through Delta-like Notch ligands. *J. Clin. Invest.* 127:1574–1588. https://doi.org/10.1172/jci89535

Chung, J., V. Radojcic, E. Perkey, T.J. Parnell, Y. Niknafs, X. Jin, A. Friedman, N. Labrecque, B.R. Blazar, T.V. Brennan, et al. 2019. Early notch signals induce a pathogenic molecular signature during priming of alloantigen-specific conventional CD4$^+$ T cells in graft-versus-host disease. *J. Immunol.* 203:557–568. https://doi.org/10.4049/jimmunol.1900192

Connolly, A., R. Panes, M. Tual, R. Lafortune, A. Bellemare-Pelletier, and E. Gagnon. 2021. TMEM16F mediates bystander TCR-CD3 membrane dissociation at the immunological synapse and potentiates T cell activation. *Sci. Signal.* 14:eabb5146. https://doi.org/10.1126/scisignal.abb5146

Cremasco, V., M.C. Woodruff, L. Onder, J. Cupovic, J.M. Nieves-Bonilla, F.A. Schildberg, J. Chang, F. Cremasco, C.J. Harvey, K. Wucherpfennig, et al. 2014. B cell homeostasis and follicle confines are governed by fibroblastic reticular cells. *Nat. Immunol.* 15:973–981. https://doi.org/10.1038/ni.2965

Cupovic, J., S.S. Ring, L. Onder, J.M. Colston, M. Lütge, H.-W. Cheng, A. De Martin, N.M. Provine, L. Flatz, A. Oxenius, et al. 2021. Adenovirus vector vaccination reprograms pulmonary fibroblastic niches to support protective inflating memory CD8$^+$ T cells. *Nat. Immunol.* 22:1042–1051. https://doi.org/10.1038/s41590-021-00969-3

De Martin, A., Y. Stanossek, M. Lütge, N. Cadosch, L. Onder, H.-W. Cheng, J.D. Brandstadter, I. Maillard, S.J. Stoeckli, N.B. Pikor, and B. Ludewig. 2023. PI16$^+$ reticular cells in human palatine tonsils govern T cell activity in distinct subepithelial niches. *Nat. Immunol.* 24:1138–1148. https://doi.org/10.1038/s41590-023-01502-4

Dennis, G. Jr., B.T. Sherman, D.A. Hosack, J. Yang, W. Gao, H.C. Lane, and R.A. Lempicki. 2003. DAVID: Database for annotation, visualization, and integrated discovery. *Genome Biol.* 4:P3.

Dobin, A., C.A. Davis, F. Schlesinger, J. Drenkow, C. Zaleski, S. Jha, P. Batut, M. Chaisson, and T.R. Gingeras. 2013. STAR: Ultrafast universal RNA-seq aligner. *Bioinformatics*. 29:15–21. https://doi.org/10.1093/bioinformatics/bts635

Dominguez, C.X., R.A. Amezquita, T. Guan, H.D. Marshall, N.S. Joshi, S.H. Kleinstein, and S.M. Kaech. 2015. The transcription factors ZEB2 and T-bet cooperate to program cytotoxic T cell terminal differentiation in response to LCMV viral infection. *J. Exp. Med.* 212:2041–2056. https://doi.org/10.1084/jem.20150186

Fasnacht, N., H.-Y. Huang, U. Koch, S. Favre, F. Auderset, Q. Chai, L. Onder, S. Kallert, D.D. Pinschewer, H.R. MacDonald, et al. 2014. Specific fibroblastic niches in secondary lymphoid organs orchestrate distinct Notch-regulated immune responses. *J. Exp. Med.* 211:2265–2279. https://doi.org/10.1084/jem.20132528

Fiorini, E., E. Merck, A. Wilson, I. Ferrero, W. Jiang, U. Koch, F. Auderset, E. Laurenti, F. Tacchini-Cottier, M. Pierres, et al. 2009. Dynamic regulation of notch 1 and notch 2 surface expression during T cell development and activation revealed by novel monoclonal antibodies. *J. Immunol.* 183:7212–7222. https://doi.org/10.4049/jimmunol.0902432

Gene Ontology Consortium. 2021. The Gene Ontology resource: Enriching a GOld mine. *Nucleic Acids Res.* 49:D325–D334. https://doi.org/10.1093/nar/gkaa1113

Guan, T., C.X. Dominguez, R.A. Amezquita, B.J. Laidlaw, J. Cheng, J. Henao-Mejia, A. Williams, R.A. Flavell, J. Lu, and S.M. Kaech. 2018. ZEB1, ZEB2, and the miR-200 family form a counterregulatory network to regulate CD8$^+$ T cell fates. *J. Exp. Med.* 215:1153–1168. https://doi.org/10.1084/jem.20171352

Heinz, S., C. Benner, N. Spann, E. Bertolino, Y.C. Lin, P. Laslo, J.X. Cheng, C. Murre, H. Singh, and C.K. Glass. 2010. Simple combinations of lineage-determining transcription factors prime cis-regulatory elements required for macrophage and B cell identities. *Mol. Cell.* 38:576–589. https://doi.org/10.1016/j.molcel.2010.05.004

Hogquist, K.A., S.C. Jameson, W.R. Heath, J.L. Howard, M.J. Bevan, and F.R. Carbone. 1994. T cell receptor antagonist peptides induce positive selection. *Cell.* 76:17–27. https://doi.org/10.1016/0092-8674(94)90169-4

Hombrink, P., C. Helbig, R.A. Backer, B. Piet, A.E. Oja, R. Stark, G. Brasser, A. Jongejan, R.E. Jonkers, B. Nota, et al. 2016. Programs for the persistence, vigilance and control of human CD8$^+$ lung-resident memory T cells. *Nat. Immunol.* 17:1467–1478. https://doi.org/10.1038/ni.3589

Huang, W., B.T. Sherman, and R.A. Lempicki. 2009. Bioinformatics enrichment tools: Paths toward the comprehensive functional analysis of large gene lists. *Nucleic Acids Res.* 37:1–13. https://doi.org/10.1093/nar/gkn923

Huang, H., P. Zhou, J. Wei, L. Long, H. Shi, Y. Dhungana, N.M. Chapman, G. Fu, J. Saravia, J.L. Raynor, et al. 2021. In vivo CRISPR screening reveals

nutrient signaling processes underpinning CD8+ T cell fate decisions. *Cell*. 184:1245–1261.e21. https://doi.org/10.1016/j.cell.2021.02.021

Ichii, H., A. Sakamoto, M. Hatano, S. Okada, H. Toyama, S. Taki, M. Arima, Y. Kuroda, and T. Tokuhisa. 2002. Role for Bcl-6 in the generation and maintenance of memory CD8+ T cells. *Nat. Immunol.* 3:558–563. https://doi.org/10.1038/ni802

Intlekofer, A.M., N. Takemoto, E.J. Wherry, S.A. Longworth, J.T. Northrup, V.R. Palanivel, A.C. Mullen, C.R. Gasink, S.M. Kaech, J.D. Miller, et al. 2005. Effector and memory CD8+ T cell fate coupled by T-bet and eomesodermin. *Nat. Immunol.* 6:1236–1244. https://doi.org/10.1038/ni1268

Ito, T., M. Schaller, C.M. Hogaboam, T.J. Standiford, M. Sandor, N.W. Lukacs, S.W. Chensue, and S.L. Kunkel. 2009. TLR9 regulates the mycobacteria-elicited pulmonary granulomatous immune response in mice through DC-derived Notch ligand delta-like 4. *J. Clin. Invest.* 119:33–46. https://doi.org/10.1172/jci35647

Ji, Y., Z. Pos, M. Rao, C.A. Klebanoff, Z. Yu, M. Sukumar, R.N. Reger, D.C. Palmer, Z .A. Borman, P. Muranski, et al. 2011. Repression of the DNA-binding inhibitor Id3 by Blimp-1 limits the formation of memory CD8+ T cells. *Nat. Immunol.* 12:1230–1237. https://doi.org/10.1038/ni.2153

Joshi, N.S., W. Cui, A. Chandele, H.K. Lee, D.R. Urso, J. Hagman, L. Gapin, and S.M. Kaech. 2007. Inflammation directs memory precursor and short-lived effector CD8(+) T cell fates via the graded expression of T-bet transcription factor. *Immunity*. 27:281–295. https://doi.org/10.1016/j.immuni.2007.07.010

Kadam, S., and B.M. Emerson. 2003. Transcriptional specificity of human SWI/SNF BRG1 and BRM chromatin remodeling complexes. *Mol. Cell*. 11:377–389. https://doi.org/10.1016/s1097-2765(03)00034-0

Kaech, S.M., J.T. Tan, E.J. Wherry, B.T. Konieczny, C.D. Surh, and R. Ahmed. 2003. Selective expression of the interleukin 7 receptor identifies effector CD8 T cells that give rise to long-lived memory cells. *Nat. Immunol.* 4:1191–1198. https://doi.org/10.1038/ni1009

Kakaradov, B., J. Arsenio, C.E. Widjaja, Z. He, S. Aigner, P.J. Metz, B. Yu, E.J. Wehrens, J. Lopez, S.H. Kim, et al. 2017. Early transcriptional and epigenetic regulation of CD8+ T cell differentiation revealed by single-cell RNA sequencing. *Nat. Immunol.* 18:422–432. https://doi.org/10.1038/ni.3688

Kalia, V., S. Sarkar, S. Subramaniam, W.N. Haining, K.A. Smith, and R. Ahmed. 2010. Prolonged interleukin-2Ralpha expression on virus-specific CD8+ T cells favors terminal-effector differentiation in vivo. *Immunity*. 32:91–103. https://doi.org/10.1016/j.immuni.2009.11.010

Kallies, A., A. Xin, G.T. Belz, and S.L. Nutt. 2009. Blimp-1 transcription factor is required for the differentiation of effector CD8(+) T cells and memory responses. *Immunity*. 31:283–295. https://doi.org/10.1016/j.immuni.2009.06.021

Kim, E.H., J.A. Sullivan, E.H. Plisch, M.M. Tejera, A. Jatzek, K.Y. Choi, and M. Suresh. 2012. Signal integration by Akt regulates CD8 T cell effector and memory differentiation. *J. Immunol.* 188:4305–4314. https://doi.org/10.4049/jimmunol.1103568

Kurachi, M., R.A. Barnitz, N. Yosef, P.M. Odorizzi, M.A. DiIorio, M.E. Lemieux, K. Yates, J. Godec, M.G. Klatt, A. Regev, et al. 2014. The transcription factor BATF operates as an essential differentiation checkpoint in early effector CD8+ T cells. *Nat. Immunol.* 15:373–383. https://doi.org/10.1038/ni.2834

Kurd, N.S., Z. He, T.L. Louis, J.J. Milner, K.D. Omilusik, W. Jin, M.S. Tsai, C.E. Widjaja, J.N. Kanbar, J.G. Olvera, et al. 2020. Early precursors and molecular determinants of tissue-resident memory CD8+ T lymphocytes revealed by single-cell RNA sequencing. *Sci. Immunol.* 5:eaaz6894. https://doi.org/10.1126/sciimmunol.aaz6894

Laky, K., S. Evans, A. Perez-Diez, and B.J. Fowlkes. 2015. Notch signaling regulates antigen sensitivity of naive CD4+ T cells by tuning co-stimulation. *Immunity*. 42:80–94. https://doi.org/10.1016/j.immuni.2014.12.027

Langmead, B., and S.L. Salzberg. 2012. Fast gapped-read alignment with Bowtie 2. *Nat. Methods*. 9:357–359. https://doi.org/10.1038/nmeth.1923

Lewis, K.L., M.L. Caton, M. Bogunovic, M. Greter, L.T. Grajkowska, D. Ng, A. Klinakis, I.F. Charo, S. Jung, J.L. Gommerman, et al. 2011. Notch2 receptor signaling controls functional differentiation of dendritic cells in the spleen and intestine. *Immunity*. 35:780–791. https://doi.org/10.1016/j.immuni.2011.08.013

Li, B., and C.N. Dewey. 2011. RSEM: Accurate transcript quantification from RNA-seq data with or without a reference genome. *BMC Bioinformatics*. 12:323. https://doi.org/10.1186/1471-2105-12-323

Li, Z., M.H. Schulz, T. Look, M. Begemann, M. Zenke, and I.G. Costa. 2019. Identification of transcription factor binding sites using ATAC-seq. *Genome Biol.* 20:45. https://doi.org/10.1186/s13059-019-1642-2

Liao, Y., G.K. Smyth, and W. Shi. 2014. featureCounts: an efficient general purpose program for assigning sequence reads to genomic features. *Bioinformatics*. 30:923–930. https://doi.org/10.1093/bioinformatics/btt656

Liu, X., Y. Wang, H. Lu, J. Li, X. Yan, M. Xiao, J. Hao, A. Alekseev, H. Khong, T. Chen, et al. 2019. Genome-wide analysis identifies NR4A1 as a key mediator of T cell dysfunction. *Nature*. 567:525–529. https://doi.org/10.1038/s41586-019-0979-8

Love, M.I., W. Huber, and S. Anders. 2014. Moderated estimation of fold change and dispersion for RNA-seq data with DESeq2. *Genome Biol.* 15:550. https://doi.org/10.1186/s13059-014-0550-8

Macintyre, A.N., D. Finlay, G. Preston, L.V. Sinclair, C.M. Waugh, P. Tamas, C. Feijoo, K. Okkenhaug, and D.A. Cantrell. 2011. Protein kinase B controls transcriptional programs that direct cytotoxic T cell fate but is dispensable for T cell metabolism. *Immunity*. 34:224–236. https://doi.org/10.1016/j.immuni.2011.01.012

Maekawa, Y., Y. Minato, C. Ishifune, T. Kurihara, A. Kitamura, H. Kojima, H. Yagita, M. Sakata-Yanagimoto, T. Saito, I. Taniuchi, et al. 2008. Notch2 integrates signaling by the transcription factors RBP-J and CREB1 to promote T cell cytotoxicity. *Nat. Immunol.* 9:1140–1147. https://doi.org/10.1038/ni.1649

Maillard, I., A.P. Weng, A.C. Carpenter, C.G. Rodriguez, H. Sai, L. Xu, D. Allman, J.C. Aster, and W.S. Pear. 2004. Mastermind critically regulates Notch-mediated lymphoid cell fate decisions. *Blood*. 104:1696–1702. https://doi.org/10.1182/blood-2004-02-0514

Martin, A.P., G.A. Bradshaw, R.J. Eisert, E.D. Egan, L. Tveriakhina, J.M. Rogers, A.N. Dates, G. Scanavachi, J.C. Aster, T. Kirchhausen, et al. 2023. A spatiotemporal Notch interaction map from plasma membrane to nucleus. *Sci. Signal*. 16:eadg6474. https://doi.org/10.1126/scisignal.adg6474

Mathieu, M., N. Cotta-Grand, J.F. Daudelin, P. Thébault, and N. Labrecque. 2013. Notch signaling regulates PD-1 expression during CD8(+) T-cell activation. *Immunol. Cell Biol.* 91:82–88. https://doi.org/10.1038/icb.2012.53

Mathieu, M., F. Duval, J.-F. Daudelin, and N. Labrecque. 2015. The Notch signaling pathway controls short-lived effector CD8+ T cell differentiation but is dispensable for memory generation. *J. Immunol.* 194:5654–5662. https://doi.org/10.4049/jimmunol.1402837

Maurice De Sousa, D., F. Duval, J.-F. Daudelin, S. Boulet, and N. Labrecque. 2019. The Notch signaling pathway controls CD8+ T cell differentiation independently of the classical effector HES1. *PLoS One*. 14. e0215012. https://doi.org/10.1371/journal.pone.0215012

McDonald, B., B.Y. Chick, N.S. Ahmed, M. Burns, S. Ma, E. Casillas, D. Chen, T.H. Mann, C. O'Connor, N. Hah, et al. 2023. Canonical BAF complex activity shapes the enhancer landscape that licenses CD8+ T cell effector and memory fates. *Immunity*. 56:1303–1319.e5. https://doi.org/10.1016/j.immuni.2023.05.005

McLean, C.Y., D. Bristor, M. Hiller, S.L. Clarke, B.T. Schaar, C.B. Lowe, A.M. Wenger, and G. Bejerano. 2010. GREAT improves functional interpretation of cis-regulatory regions. *Nat. Biotechnol.* 28:495–501. https://doi.org/10.1038/nbt.1630

Milner, J.J., C. Toma, Z. He, N.S. Kurd, Q.P. Nguyen, B. McDonald, L. Quezada, C.E. Widjaja, D.A. Witherden, J.T. Crowl, et al. 2020. Heterogenous populations of tissue-resident CD8+ T cells are generated in response to infection and malignancy. *Immunity*. 52:808–824.e7. https://doi.org/10.1016/j.immuni.2020.04.007

Mochizuki, K., F. Xie, S. He, Q. Tong, Y. Liu, I. Mochizuki, Y. Guo, K. Kato, H. Yagita, S. Mineishi, and Y. Zhang. 2013. Delta-like ligand 4 identifies a previously uncharacterized population of inflammatory dendritic cells that plays important roles in eliciting allogeneic T cell responses in mice. *J. Immunol.* 190:3772–3782. https://doi.org/10.4049/jimmunol.1202820

Mochizuki, K., L. Meng, I. Mochizuki, Q. Tong, S. He, Y. Liu, J. Purushe, H. Fung, M.R. Zaidi, Y. Zhang, et al. 2016. Programming of donor T cells using allogeneic δ-like ligand 4-positive dendritic cells to reduce GVHD in mice. *Blood*. 127:3270–3280. https://doi.org/10.1182/blood-2015-05-644476

Mohtashami, M., D.K. Shah, H. Nakase, K. Kianizad, H.T. Petrie, and J.C. Zúñiga-Pflücker. 2010. Direct comparison of Dll1- and Dll4-mediated Notch activation levels shows differential lymphomyeloid lineage commitment outcomes. *J. Immunol.* 185:867–876. https://doi.org/10.4049/jimmunol.1000782

Napolitani, G., A. Rinaldi, F. Bertoni, F. Sallusto, and A. Lanzavecchia. 2005. Selected Toll-like receptor agonist combinations synergistically trigger a T helper type 1-polarizing program in dendritic cells. *Nat. Immunol.* 6:769–776. https://doi.org/10.1038/ni1223

Ntziachristos, P., A. Tsirigos, P. Van Vlierberghe, J. Nedjic, T. Trimarchi, M.S. Flaherty, D. Ferres-Marco, V. da Ros, Z. Tang, J. Siegle, et al. 2012. Genetic inactivation of the polycomb repressive complex 2 in T cell acute lymphoblastic leukemia. *Nat. Med.* 18:298–301. https://doi.org/10.1038/nm.2651

Obar, J.J., M.J. Molloy, E.R. Jellison, T.A. Stoklasek, W. Zhang, E.J. Usherwood, and L. Lefrançois. 2010. CD4+ T cell regulation of CD25 expression controls development of short-lived effector CD8+ T cells in primary and secondary responses. *Proc. Natl. Acad. Sci. USA.* 107:193–198. https://doi.org/10.1073/pnas.0909945107

Odagiu, L., S. Boulet, D. Maurice De Sousa, J.-F. Daudelin, S. Nicolas, and N. Labrecque. 2020. Early programming of CD8+ T cell response by the orphan nuclear receptor NR4A3. *Proc. Natl. Acad. Sci. USA.* 117:24392–24402. https://doi.org/10.1073/pnas.2007224117

Omilusik, K.D., J.A. Best, B. Yu, S. Goossens, A. Weidemann, J.V. Nguyen, E. Seuntjens, A. Stryjewska, C. Zweier, R. Roychoudhuri, et al. 2015. Transcriptional repressor ZEB2 promotes terminal differentiation of CD8+ effector and memory T cell populations during infection. *J. Exp. Med.* 212:2027–2039. https://doi.org/10.1084/jem.20150194

Onder, L., H.W. Cheng, and B. Ludewig. 2022. Visualization and functional characterization of lymphoid organ fibroblasts. *Immunol. Rev.* 306:108–122. https://doi.org/10.1111/imr.13051

Osborne, B.A., and L.M. Minter. 2007. Notch signalling during peripheral T-cell activation and differentiation. *Nat. Rev. Immunol.* 7:64–75. https://doi.org/10.1038/nri1998

Ostiguy, V., E.L. Allard, M. Marquis, J. Leignadier, and N. Labrecque. 2007. IL-21 promotes T lymphocyte survival by activating the phosphatidylinositol-3 kinase signaling cascade. *J. Leukoc. Biol.* 82:645–656. https://doi.org/10.1189/jlb.0806494

Perez-Shibayama, C., U. Islander, M. Lütge, H.-W. Cheng, L. Onder, S.S. Ring, A. De Martin, M. Novkovic, J. Colston, C. Gil-Cruz, and B. Ludewig. 2020. Type I interferon signaling in fibroblastic reticular cells prevents exhaustive activation of antiviral CD8+ T cells. *Sci. Immunol.* 5:eabb7066. https://doi.org/10.1126/sciimmunol.abb7066

Perkey, E., D. Maurice De Sousa, L. Carrington, J. Chung, A. Dils, D. Granadier, U. Koch, F. Radtke, B. Ludewig, B.R. Blazar, et al. 2020. GCNT1-Mediated O-glycosylation of the sialomucin CD43 is a sensitive indicator of notch signaling in activated T cells. *J. Immunol.* 204:1674–1688. https://doi.org/10.4049/jimmunol.1901194

Petrovic, J., Y. Zhou, M. Fasolino, N. Goldman, G.W. Schwartz, M.R. Mumbach, S.C. Nguyen, K.S. Rome, Y. Sela, Z. Zapataro, et al. 2019. Oncogenic notch promotes long-range regulatory interactions within hyperconnected 3D cliques. *Mol. Cell.* 73:1174–1190.e12. https://doi.org/10.1016/j.molcel.2019.01.006

Pillidge, Z., and S.J. Bray. 2019. SWI/SNF chromatin remodeling controls Notch-responsive enhancer accessibility. *EMBO Rep.* 20:e46944. https://doi.org/10.15252/embr.201846944

Preuße, K., L. Tveriakhina, K. Schuster-Gossler, C. Gaspar, A.I. Rosa, D. Henrique, A. Gossler, and M. Stauber. 2015. Context-dependent functional divergence of the notch ligands DLL1 and DLL4 in vivo. *PLoS Genet.* 11:e1005328. https://doi.org/10.1371/journal.pgen.1005328

Radtke, F., H.R. MacDonald, and F. Tacchini-Cottier. 2013. Regulation of innate and adaptive immunity by Notch. *Nat. Rev. Immunol.* 13:427–437. https://doi.org/10.1038/nri3445

Ramírez, F., D.P. Ryan, B. Grüning, V. Bhardwaj, F. Kilpert, A.S. Richter, S. Heyne, F. Dündar, and T. Manke. 2016. deepTools2: a next generation web server for deep-sequencing data analysis. *Nucleic Acids Res.* 44:W160–W165. https://doi.org/10.1093/nar/gkw257

Ridgway, J., G. Zhang, Y. Wu, S. Stawicki, W.-C. Liang, Y. Chanthery, J. Kowalski, R.J. Watts, C. Callahan, I. Kasman, et al. 2006. Inhibition of Dll4 signalling inhibits tumour growth by deregulating angiogenesis. *Nature.* 444:1083–1087. https://doi.org/10.1038/nature05313

Rodda, L.B., O. Bannard, B. Ludewig, T. Nagasawa, and J.G. Cyster. 2015. Phenotypic and morphological properties of germinal center dark zone Cxcl12-expressing reticular cells. *J. Immunol.* 195:4781–4791. https://doi.org/10.4049/jimmunol.1501191

Roychoudhuri, R., D. Clever, P. Li, Y. Wakabayashi, K.M. Quinn, C.A. Klebanoff, Y. Ji, M. Sukumar, R.L. Eil, Z. Yu, et al. 2016. BACH2 regulates CD8(+) T cell differentiation by controlling access of AP-1 factors to enhancers. *Nat. Immunol.* 17:851–860. https://doi.org/10.1038/ni.3441

Rutishauser, R.L., G.A. Martins, S. Kalachikov, A. Chandele, I.A. Parish, E. Meffre, J. Jacob, K. Calame, and S.M. Kaech. 2009. Transcriptional repressor Blimp-1 promotes CD8(+) T cell terminal differentiation and represses the acquisition of central memory T cell properties. *Immunity.* 31:296–308. https://doi.org/10.1016/j.immuni.2009.05.014

Sarkar, S., V. Kalia, W.N. Haining, B.T. Konieczny, S. Subramaniam, and R. Ahmed. 2008. Functional and genomic profiling of effector CD8 T cell subsets with distinct memory fates. *J. Exp. Med.* 205:625–640. https://doi.org/10.1084/jem.20071641

Satija, R., J.A. Farrell, D. Gennert, A.F. Schier, and A. Regev. 2015. Spatial reconstruction of single-cell gene expression data. *Nat. Biotechnol.* 33:495–502. https://doi.org/10.1038/nbt.3192

Schwanbeck, R. 2015. The role of epigenetic mechanisms in Notch signaling during development. *J. Cell. Physiol.* 230:969–981. https://doi.org/10.1002/jcp.24851

Schwanbeck, R., S. Martini, K. Bernoth, and U. Just. 2011. The notch signaling pathway: Molecular basis of cell context dependency. *Eur. J. Cell Biol.* 90:572–581. https://doi.org/10.1016/j.ejcb.2010.10.004

Scott-Browne, J.P., I.F. López-Moyado, S. Trifari, V. Wong, L. Chavez, A. Rao, and R.M. Pereira. 2016. Dynamic changes in chromatin accessibility occur in CD8+ T cells responding to viral infection. *Immunity.* 45:1327–1340. https://doi.org/10.1016/j.immuni.2016.10.028

Skalska, L., R. Stojnic, J. Li, B. Fischer, G. Cerda-Moya, H. Sakai, S. Tajbakhsh, S. Russell, B. Adryan, and S.J. Bray. 2015. Chromatin signatures at Notch-regulated enhancers reveal large-scale changes in H3K56ac upon activation. *EMBO J.* 34:1889–1904. https://doi.org/10.15252/embj.201489923

Skokos, D., and M.C. Nussenzweig. 2007. CD8- DCs induce IL-12-independent Th1 differentiation through Delta 4 Notch-like ligand in response to bacterial LPS. *J. Exp. Med.* 204:1525–1531. https://doi.org/10.1084/jem.20062305

Subramanian, A., P. Tamayo, V.K. Mootha, S. Mukherjee, B.L. Ebert, M.A. Gillette, A. Paulovich, S.L. Pomeroy, T.R. Golub, E.S. Lander, and J.P. Mesirov. 2005. Gene set enrichment analysis: A knowledge-based approach for interpreting genome-wide expression profiles. *Proc. Natl. Acad. Sci. USA.* 102:15545–15550. https://doi.org/10.1073/pnas.0506580102

Sugimoto, K., Y. Maekawa, A. Kitamura, J. Nishida, A. Koyanagi, H. Yagita, H. Kojima, S. Chiba, M. Shimada, and K. Yasutomo. 2010. Notch2 signaling is required for potent antitumor immunity in vivo. *J. Immunol.* 184:4673–4678. https://doi.org/10.4049/jimmunol.0903661

Takeuchi, J.K., H. Lickert, B.W. Bisgrove, X. Sun, M. Yamamoto, K. Chawengsaksophak, H. Hamada, H.J. Yost, J. Rossant, and B.G. Bruneau. 2007. Baf60c is a nuclear Notch signaling component required for the establishment of left-right asymmetry. *Proc. Natl. Acad. Sci. USA.* 104:846–851. https://doi.org/10.1073/pnas.0608118104

Tindemans, I., A. van Schoonhoven, A. KleinJan, M.J. de Bruijn, M. Lukkes, M. van Nimwegen, A. van den Branden, I.M. Bergen, O.B. Corneth, W.F. van IJcken, et al. 2020. Notch signaling licenses allergic airway inflammation by promoting Th2 cell lymph node egress. *J. Clin. Invest.* 130:3576–3591. https://doi.org/10.1172/jci128310

Tkachev, V., A. Vanderbeck, E. Perkey, S.N. Furlan, C. McGuckin, D. Gómez Atria, U. Gerdemann, X. Rui, J. Lane, D.J. Hunt, et al. 2023. Notch signaling drives intestinal graft-versus-host disease in mice and nonhuman primates. *Sci. Transl. Med.* 15:eadd1175. https://doi.org/10.1126/scitranslmed.add1175

Tran, I.T., A.R. Sandy, A.J. Carulli, C. Ebens, J. Chung, G.T. Shan, V. Radojcic, A. Friedman, T. Gridley, A. Shelton, et al. 2013. Blockade of individual Notch ligands and receptors controls graft-versus-host disease. *J. Clin. Invest.* 123:1590–1604. https://doi.org/10.1172/jci65477

Tsao, H.-W., J. Kaminski, M. Kurachi, R.A. Barnitz, M.A. DiIorio, M.W. LaFleur, W. Ise, T. Kurosaki, E.J. Wherry, W.N. Haining, and N. Yosef. 2022. Batf-mediated epigenetic control of effector CD8+ T cell differentiation. *Sci. Immunol.* 7:eabi4919. https://doi.org/10.1126/sciimmunol.abi4919

Vanderbeck, A., and I. Maillard. 2021. Notch signaling at the crossroads of innate and adaptive immunity. *J. Leukoc. Biol.* 109:535–548. https://doi.org/10.1002/jlb.1ri0520-138r

Vilimas, T., J. Mascarenhas, T. Palomero, M. Mandal, S. Buonamici, F. Meng, B. Thompson, C. Spaulding, S. Macaroun, M.-L. Alegre, et al. 2007. Targeting the NF-kappaB signaling pathway in Notch1-induced T-cell leukemia. *Nat. Med.* 13:70–77. https://doi.org/10.1038/nm1524

Wang, H., J. Zou, B. Zhao, E. Johannsen, T. Ashworth, H. Wong, W.S. Pear, J. Schug, S.C. Blacklow, K.L. Arnett, et al. 2011. Genome-wide analysis reveals conserved and divergent features of Notch1/RBPJ binding in human and murine T-lymphoblastic leukemia cells. *Proc. Natl. Acad. Sci. USA.* 108:14908–14913. https://doi.org/10.1073/pnas.1109023108

Wang, H., C. Zang, L. Taing, K.L. Arnett, Y.J. Wong, W.S. Pear, S.C. Blacklow, X.S. Liu, and J.C. Aster. 2014. NOTCH1-RBPJ complexes drive target gene expression through dynamic interactions with superenhancers.

Proc. Natl. Acad. Sci. USA. 111:705–710. https://doi.org/10.1073/pnas.1315023111

Wang, H., C. Zang, X.S. Liu, and J.C. Aster. 2015. The role of Notch receptors in transcriptional regulation. *J. Cell. Physiol.* 230:982–988. https://doi.org/10.1002/jcp.24872

Wang, D., H. Diao, A.J. Getzler, W. Rogal, M.A. Frederick, J. Milner, B. Yu, S. Crotty, A.W. Goldrath, and M.E. Pipkin. 2018. The transcription factor Runx3 establishes chromatin accessibility of cis-regulatory landscapes that drive memory cytotoxic T lymphocyte formation. *Immunity*. 48:659–674.e6. https://doi.org/10.1016/j.immuni.2018.03.028

Wu, D., E. Lim, F. Vaillant, M.-L. Asselin-Labat, J.E. Visvader, and G.K. Smyth. 2010. ROAST: Rotation gene set tests for complex microarray experiments. *Bioinformatics*. 26:2176–2182. https://doi.org/10.1093/bioinformatics/btq401

Yang, C.Y., J.A. Best, J. Knell, E. Yang, A.D. Sheridan, A.K. Jesionek, H.S. Li, R.R. Rivera, K.C. Lind, L.M. D'Cruz, et al. 2011. The transcriptional regulators Id2 and Id3 control the formation of distinct memory CD8$^+$ T cell subsets. *Nat. Immunol.* 12:1221–1229. https://doi.org/10.1038/ni.2158

Yatim, A., C. Benne, B. Sobhian, S. Laurent-Chabalier, O. Deas, J.-G. Judde, J.-D. Lelievre, Y. Levy, and M. Benkirane. 2012. NOTCH1 nuclear interactome reveals key regulators of its transcriptional activity and oncogenic function. *Mol. Cell*. 48:445–458. https://doi.org/10.1016/j.molcel.2012.08.022

Yu, B., K. Zhang, J.J. Milner, C. Toma, R. Chen, J.P. Scott-Browne, R.M. Pereira, S. Crotty, J.T. Chang, M.E. Pipkin, et al. 2017. Epigenetic landscapes reveal transcription factors that regulate CD8$^+$ T cell differentiation. *Nat. Immunol.* 18:573–582. https://doi.org/10.1038/ni.3706

Yukawa, M., S. Jagannathan, S. Vallabh, A.V. Kartashov, X. Chen, M.T. Weirauch, and A. Barski. 2020. AP-1 activity induced by co-stimulation is required for chromatin opening during T cell activation. *J. Exp. Med.* 217:e20182009. https://doi.org/10.1084/jem.20182009

Zhang, Y., T. Liu, C.A. Meyer, J. Eeckhoute, D.S. Johnson, B.E. Bernstein, C. Nusbaum, R.M. Myers, M. Brown, W. Li, and X.S. Liu. 2008. Model-based analysis of ChIP-seq (MACS). *Genome Biol.* 9:R137. https://doi.org/10.1186/gb-2008-9-9-r137

Zhang, Y., A.R. Sandy, J. Wang, V. Radojcic, G.T. Shan, I.T. Tran, A. Friedman, K. Kato, S. He, S. Cui, et al. 2011. Notch signaling is a critical regulator of allogeneic CD4$^+$ T-cell responses mediating graft-versus-host disease. *Blood*. 117:299–308. https://doi.org/10.1182/blood-2010-03-271940

Zhou, X., S. Yu, D.-M. Zhao, J.T. Harty, V.P. Badovinac, and H.-H. Xue. 2010. Differentiation and persistence of memory CD8(+) T cells depend on T cell factor 1. *Immunity*. 33:229–240. https://doi.org/10.1016/j.immuni.2010.08.002

JEM

Supplemental material

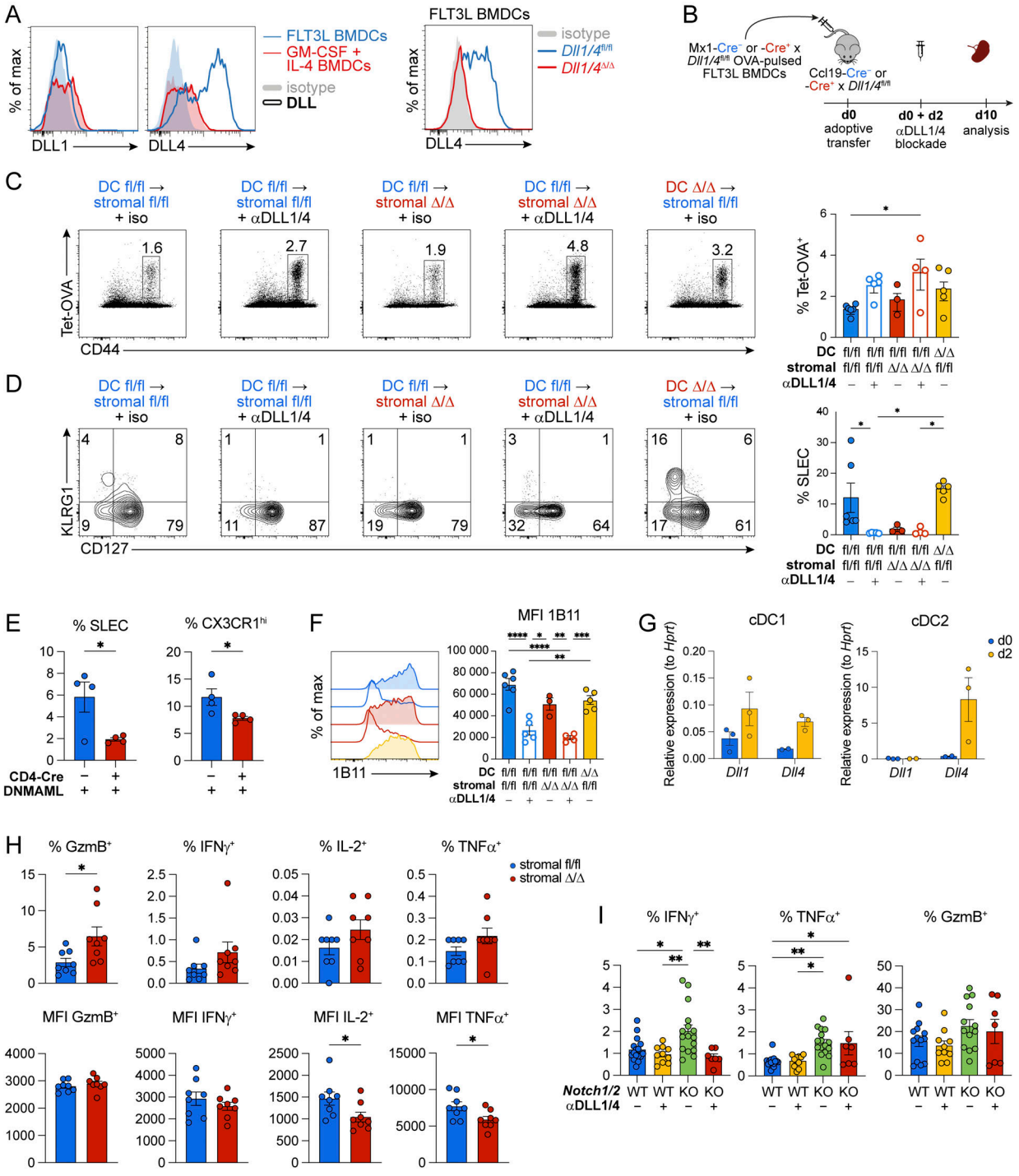

Figure S1. **Contribution of DLL1 and DLL4 to CD8⁺ T cell differentiation. (A)** Cell surface DLL1 and DLL4 expression in GM-CSF + IL-4 BMDCs (left) and FLT3L BMDCs from poly(I:C)-treated Mx1-Cre⁻ or Mx1-Cre⁺ × *Dll1/4*$^{fl/fl}$ mice (right). **(B)** Mice with or without a specific loss of Notch ligands DLL1/4 in stromal cells (Ccl19-Cre$^{+/-}$ × *Dll1*$^{fl/fl}$-*Dll4*$^{fl/fl}$) were vaccinated with OVA-loaded FLT3L BMDCs generated from poly(I:C)-treated Mx-Cre⁺ or Mx-Cre⁻ × *Dll1*$^{fl/fl}$-*Dll4*$^{fl/fl}$ mice. **(C and D)** Some mice were treated on days 0 and 2 with anti-DLL1/4 blocking antibodies. CD8⁺ T cell expansion (C) and SLEC differentiation (D) were analyzed on day 10 after vaccination. **(E)** Reduced SLEC differentiation in mice expressing DNMAML in T cells following WT DC vaccination. **(F)** 1B11 reactivity on Tet-OVA⁺ CD8⁺ T cells in mice lacking or not DLL1/4 expression on FRCs or DCs (as described in B) on day 10 after vaccination. D–F are gated on Tet-OVA⁺ CD8⁺ T cells. **(G)** On days 0 and 2 following Lm-OVA infection, cDC1 (MCHII⁺ Lin⁻ CD11c⁺ XCR1⁺) and cDC2 (MCHII⁺ Lin⁻ CD11c⁺ SIRPα⁺) were sorted. Abundance of *Dll1* and *Dll4* relative to *Hprt* transcripts was determined by RT-qPCR. **(H)** Effector functions on day 7 following Lm-OVA infection of mice with or without a specific loss of Notch ligands DLL1/4 in stromal cells (Ccl19-Cre$^{+/-}$ × *Dll1*$^{fl/fl}$-*Dll4*$^{fl/fl}$). **(I)** Effector functions of OVA-specific CD8⁺ T cells on day 7 after Lm-OVA infection with or without anti-DLL1/4 treatment. For H and I, splenocytes were briefly stimulated with the OVA peptide in the presence of Brefeldin A followed by intracellular staining. Data are from one (C–G), two (H), or three (I) independent experiments with a total of *n* = 3–13 mice per group. Error bars display means ± SEM. Ordinary one-way ANOVA with Tukey's multiple comparison was used for multiple-group comparison and unpaired two-tailed *t* test was used for two-group comparisons. *P < 0.05, **P < 0.01, ***P < 0.001, ****P < 0.0001.

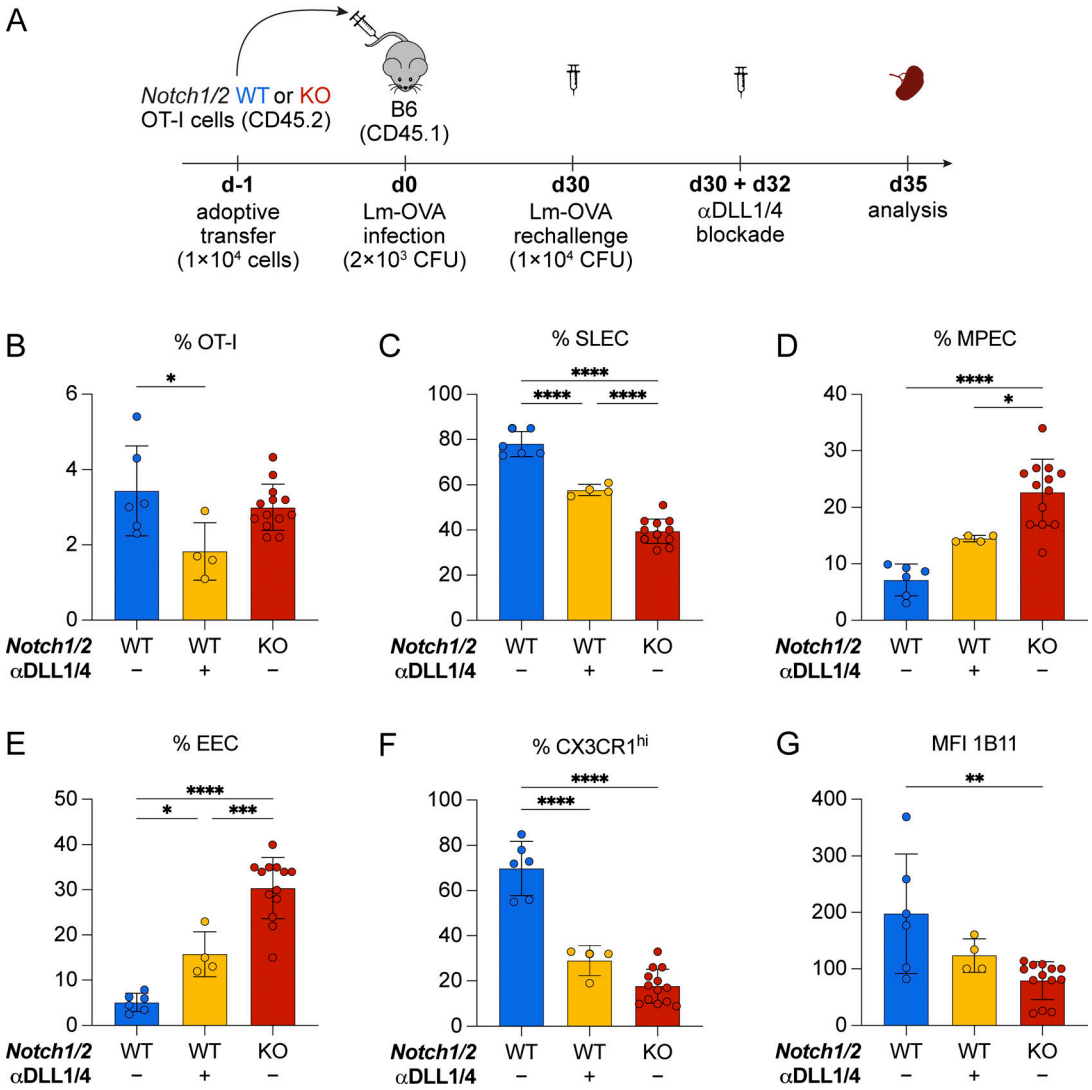

Figure S2. **SLEC differentiation of memory CD8⁺ T cells following rechallenge with Lm-OVA. (A)** Mice with memory OT-I CD8⁺ T cells (WT or Notch1/2-deficient; day 30 [d30] after Lm-OVA infection) were rechallenged with Lm-OVA and the response of secondary effectors was analyzed on day 5 after re-infection. A group of mice was treated with anti-DLL1/4 blocking antibodies on days 0 and 2 of the challenge. **(B)** Response of OT-I memory CD8⁺ T cells after rechallenge. **(C–F)** Differentiation of secondary effector OT-I T cells into SLECs (C), MPECs (D), EECs (E), and CX3CR1^{hi}CXCR3^{lo} SLECs (F). **(G)** Mean fluorescence intensity (MFI) of 1B11 on secondary effector CD8⁺ T cells. Data are from two independent experiments (A–G) of n = 4–13 mice per group. Error bars display means ± SD. Ordinary one-way ANOVA with Tukey's multiple comparison was used for multiple group comparison. *P < 0.05, **P < 0.01, ***P < 0.001, ****P < 0.0001.

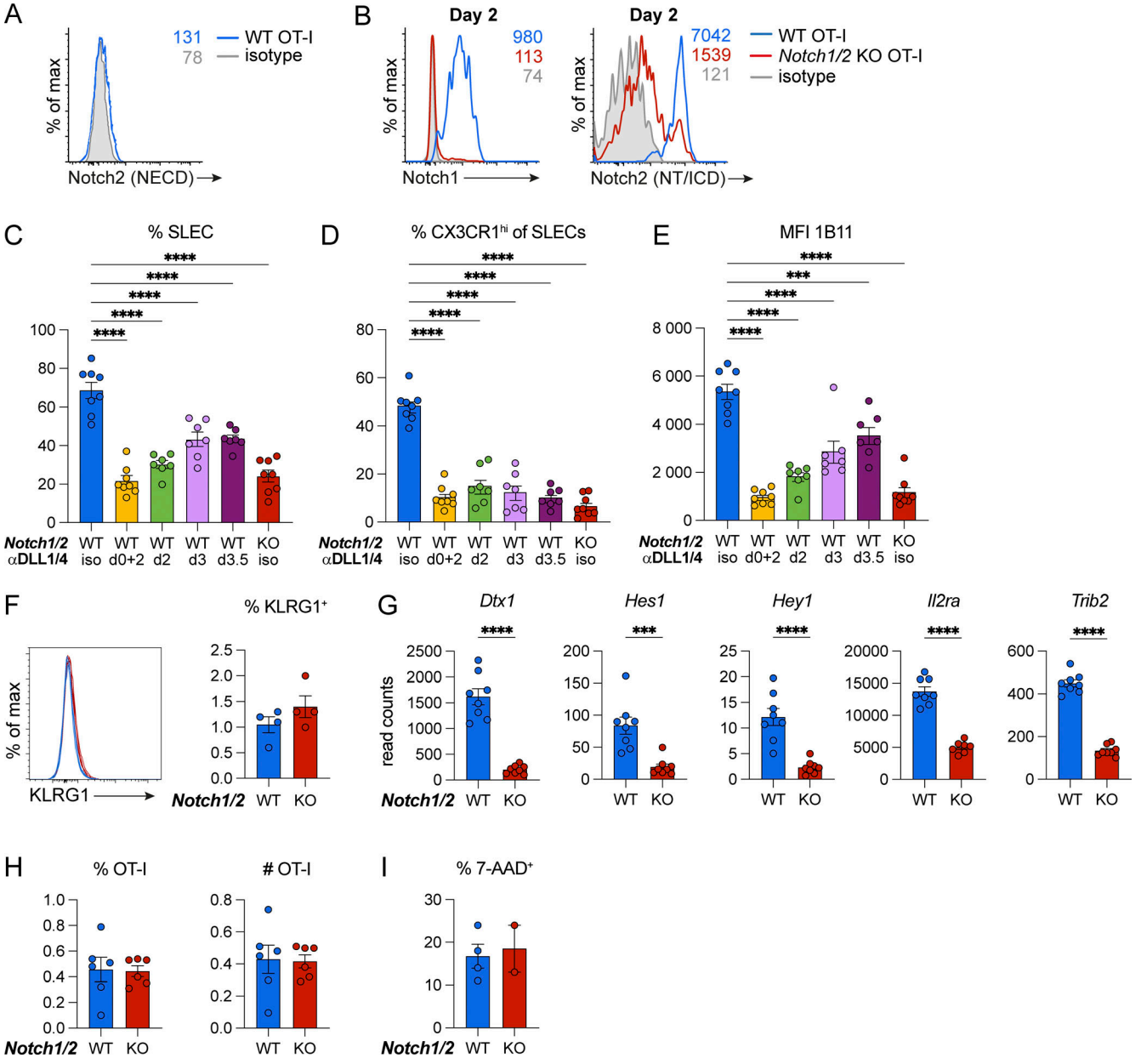

Figure S3. **Role of early Notch signaling in CD8⁺ T cells during Lm-OVA infection. (A)** Staining of the Notch2 extracellular domain in Notch1/2 WT CD8⁺ OT-I T cells on day 2 after infection with Lm-OVA. **(B)** Staining of the Notch2 transmembrane and intracellular domain in Notch1/2 WT and KO CD8⁺ OT-I T cells on day 2 after infection with Lm-OVA. **(C–E)** Proportion of SLECs (C), proportion of CX3CR1^{hi}CXCR3^{lo} SLECs (D), and MFI of 1B11 (E) from mice infected with Lm-OVA and treated with anti-DLL1/4 blocking antibodies on days (d) 0 and 2, day 2, day 3, or day 3.5. Untreated Notch1/2 WT and KO mice were used as control. **(F)** Representative histograms (left) and compilation (right) of the proportion of KLRG1⁺ cells among effector OT-I CD8⁺ T cells on day 3 after Lm-OVA infection. **(G)** Differential transcription of classical Notch target genes in the presence or absence of Notch signaling in day 3 effector CD8⁺ T cells. **(H)** Proportion and numbers of Notch1/2 WT and KO OT-I CD8⁺ T cells recovered on day 3 after infection with Lm-OVA. **(I)** Proportion of Notch1/2-deficient or sufficient OT-I CD8⁺ T cells positive for 7-AAD on day 3 after infection with Lm-OVA. Data are from one (G and J), two (C–F and I), or three (H) independent experiments with a total of n = 2–8 mice per group. Error bars display means ± SEM. Ordinary one-way ANOVA with Tukey's multiple comparisons was used for multiple group comparison and unpaired two-tailed t test was used for two-group comparisons. ***P < 0.001, ****P < 0.0001.

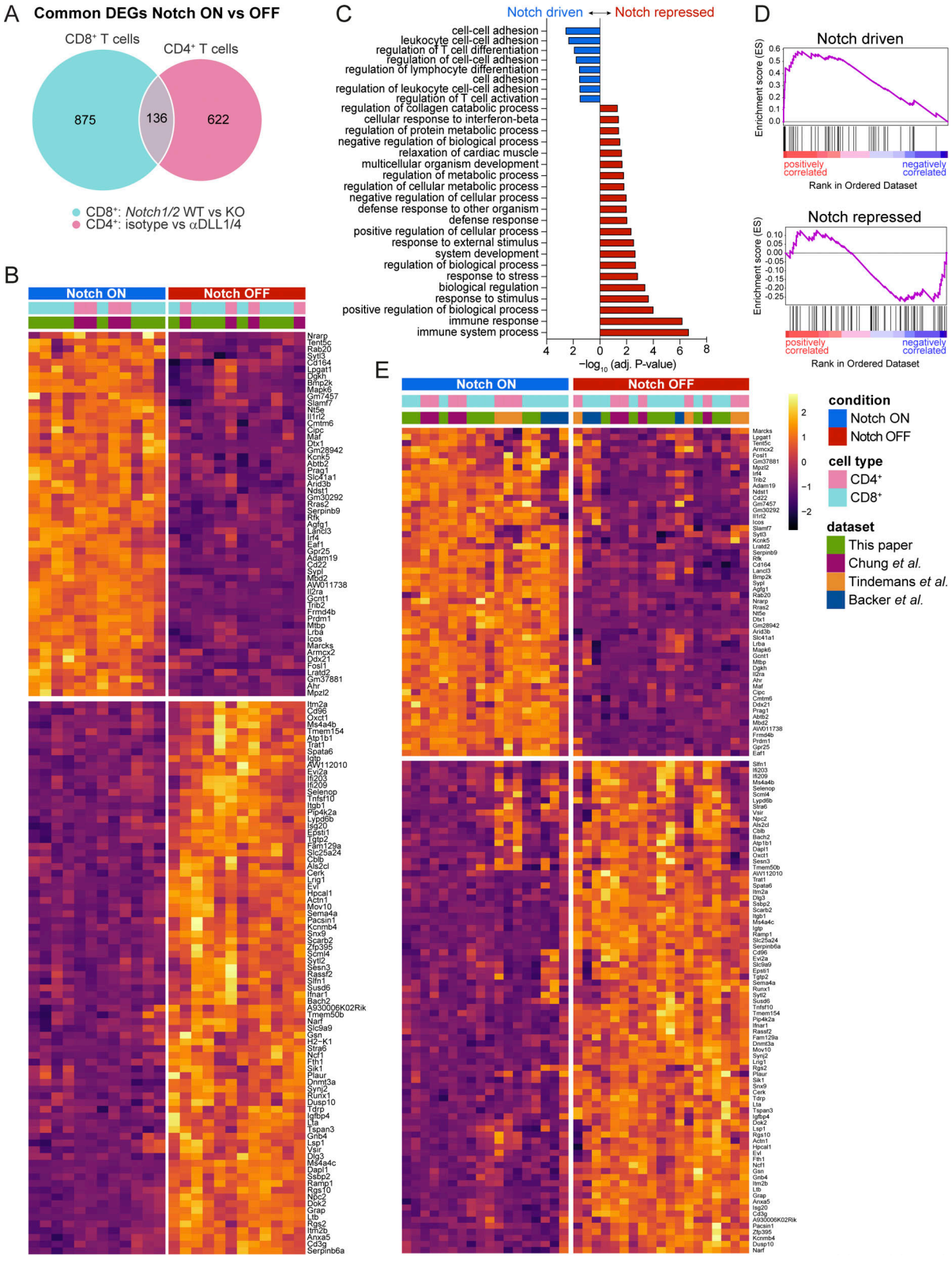

Figure S4. **Notch-T cell signature characterization and validation. (A)** Overlap of the DEGs in Notch-deprived CD4⁺ and CD8⁺ T cells. **(B)** Heatmap representation of gene expression from the T cell–specific Notch signature in CD4⁺ T cells (GSE126518) during GVHD (samples: isotype [iso] and αDLL1/4-treated) and in CD8⁺ T cells following Lm-OVA infection from this paper (samples: WT and Notch KO). **(C)** GO molecular function terms of Notch-driven or repressed signatures. **(D)** GSEA showing the enrichment of our T cell Notch signature on the DEGs from RNA-seq data comparing activated CD8⁺ T cells co-cultured on OP9 versus OP9-DLL4. **(E)** The Notch T cell signature identifies different subsets of T cells receiving Notch signals. Heatmap clustering of the different T cell subset transcriptomes using the Notch-T cell signature. Chung et al. (2019): CD4⁺ T cells early GVHD; Tindemans et al. (2020): CD4⁺ T cells Th2; Backer et al. (2014): effector CD8⁺ T cells d10 Influenza.

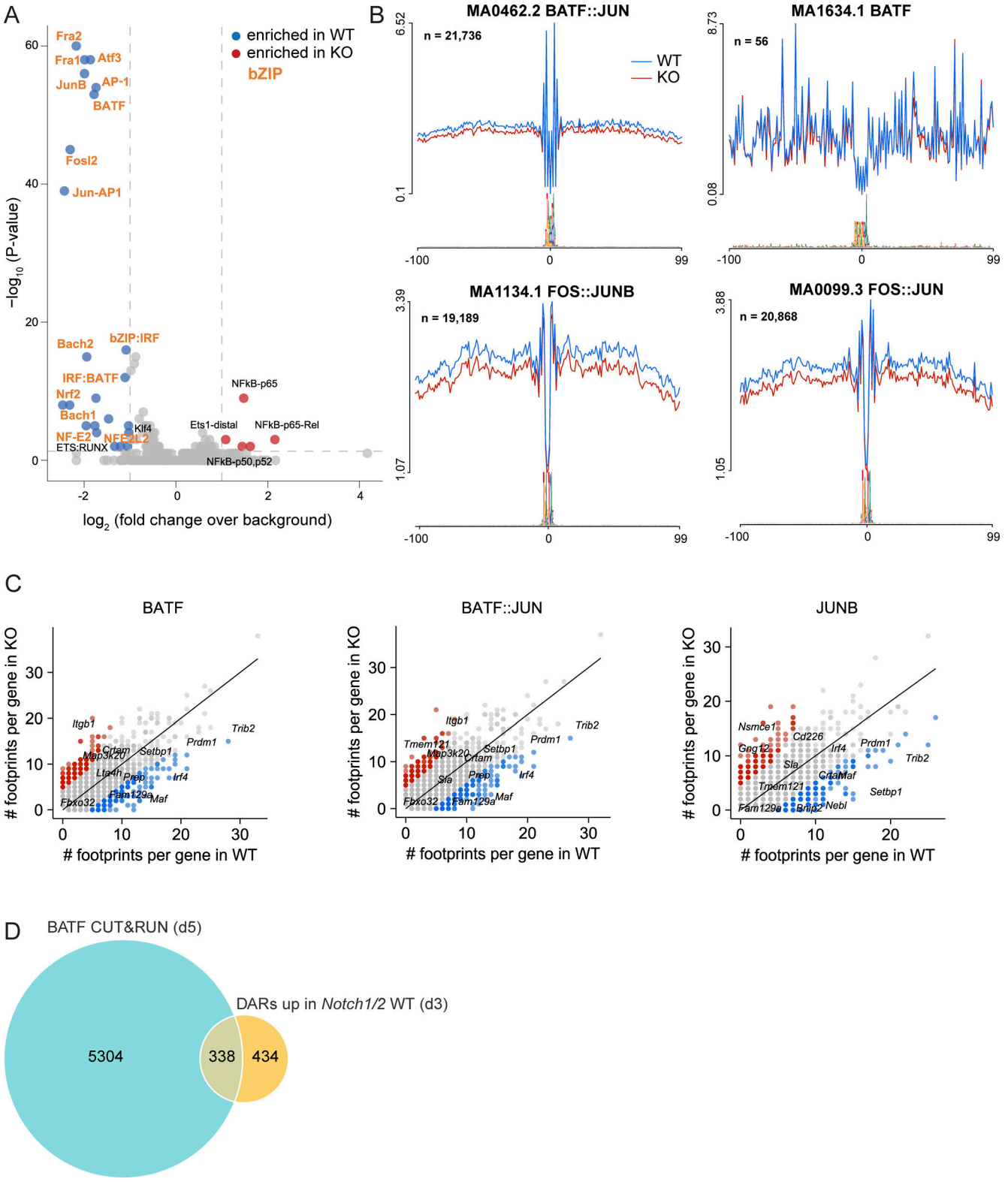

Figure S5. **Notch signaling increases the accessibility of chromatin containing motifs for bZIP transcription factors. (A)** HOMER motif enrichment analysis between Notch WT and KO DARs. bZIP transcription factors are in orange. Significant threshold was set as $P_{adj} < 0.05$ and $|\log_2 FC| > 1$. **(B)** Footprints of bZIP transcription factors. **(C)** Enrichment of bZIP transcription factor footprints with Notch-regulated DEGs. **(D)** Overlap of BATF bound genes from in vivo day 5 $CD8^+$ effectors and Notch DARs from day 3 $CD8^+$ effectors.

Provided online are Table S1, Table S2, Table S3, and Table S4. Table S1 shows the 217 differentially expressed genes (Padj ≤0.05 and |fold change| >1.5) between *Notch1/2* WT and KO CD8$^+$ T cells. Table S2 shows the 136 genes included in the T-cell Notch transcriptional signature. Table S3 shows the mROAST enrichment analysis results of the Notch T cell signature against other published datasets. Table S4 shows the complete list of antibodies used in this article.